https://doi.org/10.5194/acp-2019-689
Preprint. Discussion started: 12 November 2019

Atmospheric Chemistry and Physics Discussions

Quantification and evaluation of atmospheric ammonia emissions with different methods: A case study for the Yangtze River Delta region, China

Yu Zhao[1,2*], Mengchen Yuan[1], Xin Huang[3], Feng Chen[4], Jie Zhang[4]

1. State Key Laboratory of Pollution Control & Resource Reuse and School of the Environment, Nanjing University, 163 Xianlin Ave., Nanjing, Jiangsu 210023, China

2. Jiangsu Collaborative Innovation Center of Atmospheric Environment and Equipment Technology (CICAEET), Nanjing University of Information Science & Technology, Jiangsu 210044, China

3. School of Atmospheric Science, Nanjing University, 163 Xianlin Ave., Nanjing, Jiangsu 210023, China

4. Jiangsu Provincial Academy of Environmental Science, 176 North Jiangdong Rd., Nanjing, Jiangsu 210036, China

*Corresponding author: Yu Zhao

Phone: 86-25-89680650; email: yuzhao@nju.edu.cn

https://doi.org/10.5194/acp-2019-689
Preprint. Discussion started: 12 November 2019

Atmospheric Chemistry and Physics Discussions

Abstract

To explore the effects of data and method on emission estimation, two inventories of NH_3 emissions of the Yangtze River Delta (YRD) region in eastern China were developed for 2014 based on the constant emission factors (E1) and those characterizing the agricultural processes (E2), respectively. The latter integrated the detailed information of soil, meteorology and agricultural processes, and derived the monthly information of emission factors and activity data. The total emissions were calculated at 1765 and 1067 Gg, respectively, and agricultural activities (livestock farming and fertilizer use) were estimated to contribute 74-84% to total emissions in the two inventories. Clear differences existed in seasonal and spatial distributions of NH_3 emissions. Elevated emissions were found in March and September in E2, attributed largely to the increased top dressing fertilization and to the enhanced NH_3 volatilization under high temperature, respectively. Relatively large discrepancy between the methods existed in northern Yangtze River Delta areas with abundant croplands. The two inventories were evaluated through air quality modeling and available ground and satellite observation. With the estimated emissions 38% smaller in E2, the average of simulated NH_3 concentrations using E2 was 27% smaller than that using E1 at two ground observation sites in the YRD region. At the suburban SHPD site, the simulated NH_3 concentrations with E1 were generally larger than observation, and the modeling performance was largely improved indicated by the smaller NMEs when E2 was applied. In contrast, very limited improvement was found at the urban site JSPAES, as E2 failed to improve the emission estimation of local sources including transportation and residential activities. Compared to NH_3, the modeling performance for inorganic aerosols was better for most cases, and the differences between the simulated concentrations with E1 and E2 were clearly smaller, at 7%, 3% and 12% (relative to E1) for NH_4^+, SO_4^{2-}, and NO_3^-, respectively. Regarding the satellite-derived NH_3 column, application of E2 significantly corrected the overestimation in vertical column density simulation for January and October with E1, but did not improve the model performance for July. The NH_3 emissions might be underestimated with the assumption of linear correlation between NH_3 volatilization and soil pH for acidic soil, particularly in warm seasons. Three additional cases, i.e., 40% abatement of SO_2, 40% abatement of NO_X, and 40% abatement of both species were applied to test the sensitivity of NH_3 and inorganic aerosol concentrations to

https://doi.org/10.5194/acp-2019-689
Preprint. Discussion started: 12 November 2019

Atmospheric Chemistry and Physics Discussions

precursor emissions. Under an NH_3-rich condition for most of YRD, estimation of SO_2 emissions was detected to be more effective on simulation of secondary inorganic aerosols compared to NH_3. Reduced SO_2 would restrain the formation of $(NH_4)_2SO_4$, and thereby enhance the NH_3 concentrations. Besides the emissions, uncertainties existed as well in the limitations of ground and satellite observation and incomplete mechanism of gas to particle conversion applied in the model. To improve the air quality more effectively and efficiently, NH_3 emissions should be substantially controlled along with SO_2 and NO_X in the future.

1. Introduction

As the most important alkaline composition in the atmosphere, ammonia (NH_3) exerts crucial influences on atmospheric chemistry and nitrogen cycle. NH_3 participates in chemical reactions with sulfur dioxide (SO_2) and nitrogen oxides (NO_X), and contributes to formation of secondary inorganic aerosols (SIA) including sulfate (SO_4^{2-}), nitrate (NO_3^-), and ammonium (NH_4^+) and to thereby the elevated concentrations of fine particulate matters (PM). In the developed regions in eastern China, for example, SIA was observed to account for over 50% of $PM_{2.5}$ mass concentrations (Yang et al., 2011; Zhang et al., 2012; Huang et al., 2014), and NH_3 emissions were estimated to contribute 8-11% of $PM_{2.5}$ (Wang et al., 2011). Recent studies reported that existence of NH_3 could accelerate the heterogeneous oxidation of SO_2 and thereby sulfate formation by neutralizing aerosol acidity (Wang et al., 2016; Cheng et al., 2016; Paulot et al., 2017). Deposition of gaseous NH_3 and NH_4^+ aerosol results in soil acidification and water eutrophication. Reduced nitrogen (NH_3+NH_4^+) was monitored to contribute over 70% of total nitrogen deposition in China, revealing the importance of NH_3 on ecosystem (Pan et al., 2012). Along with the improved controls of SO_2 and NO_X emissions, enhanced contribution of NH_3 emissions was found to secondary aerosol formation and nitrogen deposition for recent years in China (Liu et al., 2013; Fu et al., 2017; Pan et al., 2018).

Quantification of NH_3 sources helps better understanding its atmospheric and ecosystem effects. In contrast to SO_2 and NO_X that are largely from industrial plants, NH_3 comes mainly from agricultural activities that are more difficult to track, including livestock farming and fertilizer use, and relatively large uncertainty in NH_3 emission inventories existed. Given the intensive agriculture across the country,

https://doi.org/10.5194/acp-2019-689
Preprint. Discussion started: 12 November 2019


Atmospheric Chemistry and Physics Discussions

various methods were developed to estimate China's NH_3 emissions at the national level for last twenty years, but clear discrepancies existed between studies, as summarized by Zhang et al. (2018). With meteorology, soil property, the method of fertilizer application and different processes of manure management considered in emission factor (emissions per unit level of activity) determination, in particular, the national NH_3 emissions estimated by Peking University group (Huang et al., 2012; Kang et al., 2016) was 39-46% smaller than those by Tsinghua University group (Dong et al., 2010; Zhao et al., 2013). Emissions of certain sectors differed significantly between various methods. For example, Zhao et al. (2013) and Kurokawa et al. (2013) calculated China's NH_3 emissions from fertilizer use at 9.5-9.8 Tg, over three times of the estimation by Kang et al. (2016). With a fertilizer modeling system that couples an air quality model and an agro-ecosystem model, Fu et al. (2015) made an estimate at 3.0 Tg, similar with Kang et al. (2016). Besides the annual emission level, discrepancies existed as well in the inter-annual trend of emissions. Kang et al. (2016) estimated that the national NH_3 emissions reached peak in 1996 and declined, while Zhang et al. (2017) and Kurokawa et al. (2013) expected a continuous growth till 2008 and 2015, respectively. The growth in NH_3 emissions got supported by satellite observation. Based on the measurement of Atmospheric Infrared Sounder (AIRS), for example, Warner et al. (2017) suggested an annual increasing rate of NH_3 concentrations at 2.3% from 2002 to 2016 in China, and it was partly attributed to the elevated emissions from fertilizer use.

Although varied methods and data resulted in discrepancies between inventories and big uncertainty in NH_3 emission estimation, very little attention has been paid to those discrepancies and the underlying reasons. At regional scale, in particular, inclusion of high-resolution information on meteorology and land use would potentially improve the spatial and seasonal distribution of agricultural NH_3 emissions in the inventory. Moreover, few studies were conducted to carefully evaluate NH_3 emission inventories incorporating air quality model and available ground and satellite observations. One possible reason is the lack of sufficient ground observation data on NH_3 and NH_4^+ aerosols open to public, as they are currently not regulated air pollutants in China and thus not regularly monitored by the government. In addition, uncertainty also existed in satellite observation on NH_3 columns and the retrieved data needs further validation (van Damme et al., 2015). Without comparison of different inventories in details and appropriate assessment based on model performance, the

https://doi.org/10.5194/acp-2019-689
Preprint. Discussion started: 12 November 2019

Atmospheric Chemistry and Physics Discussions

limitations of current emission estimates and the future steps for inventory improvement remained unclear.

In this study, therefore, we chose the Yangtze River Delta (YRD) region to develop and evaluate high-resolution emission inventories of NH_3 with different methods and data sources. Located in the eastern China, the YRD region contains the city of Shanghai and the provinces of Jiangsu, Zhejiang and Anhui (see Figure 1 for its location and prefectural cities), and is one of China's most developed and heavy-polluted regions (Xiao et al., 2011; Cheng et al., 2013; Guo et al., 2017). It is an important area of agriculture production, and was identified as a "NH_3-rich" region regarding the SIA formation (Wang et al., 2011). We developed NH_3 emission inventories for 2014 based on the constant emission factors (Method 1) and those characterizing the agricultural processes (Method 2). The two inventories were compared against each other to reveal the differences in spatial and seasonal patterns of NH_3 emissions and their origins. Evaluation of the two inventories was further conducted using a Models-3 Community Multi-scale Air Quality (CMAQ) system and available observations from ground station and satellite. Environmental parameters that might influence NH_3 simulation were identified through the model performance. Finally, the effects of SO_2 and NOx emission estimates on NH_3 and NH_4^+ aerosol simulation were evaluated through sensitivity analysis, and the policy implication of air quality improvement were accordingly suggested.

2. Data and methods

2.1 Emission inventory based on constant emission factors (E1)

The annual NH_3 emissions of the YRD region for 2014 were estimated with a bottom-up method based on constant emission factors. The inventory contained eight source categories, i.e., fertilizer application, livestock/poultry breeding, fuel combustion, biomass burning, transportation, sewage/waste treatment, industrial process, and human metabolization (see Table 1 for details). The emissions were calculated by prefectural city with the Eq. 1:

$$E_{i,j} = \sum_j \left(AL_{i,j} \times EF_j \times 10^{-3} \right) \quad (1)$$

where E is the emissions, metric ton (t); i and j indicate the prefectural city and source type, respectively; AL is the activity level, which indicated the amount of livestock,

https://doi.org/10.5194/acp-2019-689
Preprint. Discussion started: 12 November 2019


Atmospheric Chemistry and Physics Discussions

the amount of used fertilizer, the fuel burned or the industrial production, depending on the source type; and *EF* is the emission factor, kg-NH_3/unit *AL*.

Activity data were mainly taken or estimated from official statistics at the prefectural city (if available) or provincial level. For livestock/poultry breeding, the year-end stock and slaughtered numbers were used respectively for animals with the breeding cycle more and less than one year. If the city-level stock was unavailable, the output of livestock products by prefectural city was applied as the scaling factor to calculate the number from the provincial data. Table S1 in the supplement summarizes the annual numbers of livestock and poultry by prefectural city in YRD. The amount of fertilizer using by prefectural city and type was calculated as the product of sown area of cropland and fertilizer rate per unit area of cropland. The sown area by crop type was taken from city-level statistics, and the application rate by fertilizer type was obtained at provincial level from a national investigation by NDRC (2015). The detailed results of fertilizer activity data are summarized in Table S2 in the supplement. As can be seen as well in the table, the aggregated amount of fertilizer using by province were close to the provincial-level statistics, and the deviation relevant to the official statistics was 2.3% for the whole YRD. The methods and data sources for activity levels of other source categories were provided in our previous studies (Zhou et al., 2017; Zhao et al., 2017; Yang and Zhao, 2019).

The NH_3 emission factors were obtained based on a thorough literature review and summarized by source category in Table S3 in the supplement. The results from domestic field measurements were preferentially selected. For sources without suitable domestic measurements, the emission factors were also obtained from previous inventories that shared similar studying period with this work. The values from US and Europe, e.g., AP-42 database (USEPA, 2002) and the EMEP/EEA guidebook (EEA, 2013), were adopted as well when above information was lacking.

The monthly distribution of emissions by source was taken from domestic investigations in YRD (Li, 2012; Zhao et al., 2015; Zhou et al., 2017). For the purpose of air quality modeling, the emissions by sector were allocated into a grid system with a horizontal resolution at 9×9 km based on selected proxies. Those proxies included the distribution of land use (for fertilization), density of total population (for human metabolization and sewage/waste treatment) and rural population (for livestock/poultry breeding and residential solid fuel burning), gross domestic product (for industrial fuel combustion and processes), road net (for transportation), and the

https://doi.org/10.5194/acp-2019-689
Preprint. Discussion started: 12 November 2019


Atmospheric Chemistry and Physics Discussions

satellite-derived fire points from Moderate Resolution Imaging Spectroradiometer (for open biomass burning).

2.2 The method characterizing the agricultural processes (Method 2)

The emissions from fertilizer use and livestock/poultry breeding were corrected or recalculated integrating the detailed regional information of soil, meteorology and agricultural processes, as described below.

2.2.1 Fertilizer use

The growing seasons of crops affects the temporal distribution of fertilizer use and thereby that of NH_3 emissions. We investigated the growing and farming cycles by crop type in YRD from the regional farming database by the Ministry of Agriculture (MOA, http://202.127.42.157/moazzys/nongshi.aspx) and other publication (Zhang et al., 2009), and corrected the monthly amount of fertilizer using by prefectural city and fertilizer type combining the information of farming season and annual fertilizer using as given in Table S2.

Emission factors of fertilization were expected to be influenced by soil acidity, temperature, and the fertilization rate. We assumed a near-linear correlation between the soil pH and NH_3 volatilization rate (Huang et al., 2012), and calculated the emission factors of two fertilization types (basal dressing and top dressing) with Eq. 2 and 3, respectively:

$$EF_{base} = [(a_{pH} \times pH + b_{pH}) + (T_{base} - T_0 - 273.15) \times k_T] \times CF_{rate} \times CF_{method} \quad (2)$$

$$EF_{top} = [(a_{pH} \times pH + b_{pH}) + (T_{top} - T_0 - 273.15) \times k_T] \times CF_{rate} \quad (3)$$

where EF_{basal} and EF_{top} are the emission factors for basal dressing and top dressing, respectively; a_{pH} and b_{pH} are the corrected slope and intercept depending on soil pH; T_0 and k_T are the reference temperature and corrected slope depending on temperature, respectively; T_{basal} and T_{top} are the temperature of basal dressing and top dressing, respectively; and CF_{rate} and CF_{method} are the corrected factors for fertilization rate and method, respectively.

The spatial distribution of soil pH at a horizontal resolution of 1×1km was obtained from a world soil database by International Institute for Applied Systems and Analysis (IIASA, http://webarchive.iiasa.ac.at/Research/LUC/External-World-soil-database/HTML/). The correlation data between temperature and NH_3 volatilization rate were obtained from EEA (2013). T_{basal} and T_{top} were determined combining the information of

https://doi.org/10.5194/acp-2019-689
Preprint. Discussion started: 12 November 2019

Atmospheric Chemistry and Physics Discussions

farming season by MOA and the daily temperature data from European Centre for Medium-Range Weather Forecasts (ECNWF, http://apps.ecmwf.int/datasets/data/interim-full-daily/levtype=sfc/#userconsent#). All the relevant data for emission factor correction were summarized in Table S4 in the supplement. The corrected NH_3 volatilization rates of urea and ammonium bicarbonate (ABC), the mostly applied two types of fertilizer over the YRD region, were illustrated by season in Figure S1 in the supplement. Larger volatilization rates were found in northern YRD for both fertilizer types, consistent with the distribution of soil pH across the region. Taking urea as an example, the volatilization rates in April and October were commonly smaller than the uniform value applied in E1 at 17.4%, while those in July were larger. This discrepancy came partly from the consideration of fertilization types in E2. In April and October, basal dressing fertilization was commonly applied at the soil depth of 15-20 centimeters, restraining the NH_3 volatilization. In contrast, the relatively high temperature and top dressing fertilization conducted in July elevated the NH_3 volatilization.

Through the methodology mentioned above, the gridded emission factors and monthly activity levels were obtained to improve the spatial and temporal distributions of NH_3 emissions from fertilization. Figure 2 compares the activity data of fertilization between the two methods (E1 and E2), indicated by the relative deviation (*RD*):

$$RD = (E_1 - E_2)/(E_1 + E_2)/2 \quad (4)$$

In January and July, top dressing fertilization was conducted with limited crop types like rape, corn and paddy rice, while considerable basal dressing fertilization was investigated in April and October. Inclusion of those details in E2 resulted in smaller estimates of fertilizer use in winter and summer but larger in spring and autumn compared to E1.

2.2.2 Livestock/poultry breeding

In contrast to Method 1 that calculated the NH_3 emissions based on livestock numbers and annual EFs, a mass-flow approach was applied in Method 2 considering the nitrogen transformation at different stages of manure management (Beusen et al., 2008; Huang et al., 2012; EEA, 2013). Commonly applied at global or national scale, the approach calculated NH_3 emissions of manure management processes from a pool of total ammoniacal nitrogen (TAN) for three main raising systems, as shown in

https://doi.org/10.5194/acp-2019-689
Preprint. Discussion started: 12 November 2019

Atmospheric Chemistry and Physics Discussions

Figure S2 in the supplement. In YRD region, only intensive and free-range systems were considered, and the TAN was calculated by livestock/poultry type based on the breeding duration, the amount and nitrogen contents of urine/feces, and the mass fraction of TAN. The parameters were taken from Yang (2008) and Huang et al (2012), as summarized in Table S5 in the supplement. According to the nitrogen flow and phase of manure management, the activity levels were then classified into seven categories, including outdoor, housing (solid), housing (liquid), storage (solid), storage (liquid), spreading (solid) and spreading (liquid). NH_3 emissions from livestock are calculated as the product of TAN of each category and corresponding emission factors. As provided in Table S6 in the supplement, the temperature-dependant emission factors by stage/phase were taken from EEA (2013) and Huang et al. (2012), and the gridded emission factors can then be derived over the YRD region combining the meteorology data from ECNWF.

2.3 Configuration of air quality modeling

The Models-3 Community Multi-scale Air Quality (CMAQ) version 4.7.1 was applied to evaluate the NH_3 emission inventories for YRD. CMAQ is a three-dimensional Eulerian model designed for understanding the complex interactions of atmospheric chemistry and physics (http://www.cmaq-model.org). The model has been widely applied and tested in China (Qin et al., 2015; Zhou et al., 2017; Zheng et al., 2019). As shown in Figure 1, two nested domains were applied with the spatial resolutions of 27 and 9 km respectively, on a Lambert Conformal Conic projection centered at (110°E, 34°N). The mother domain (D1, 177×127 cells) covered most parts of China, and the second domain (D2, 118×121 cells) covered the whole YRD region. The two inventories of YRD NH_3 emissions developed in this work were applied in D2. Emissions from other pollutants of anthropogenic origin in D1 and D2 outside Jiangsu were obtained from the Multi resolution Emission Inventory for China (MEIC, http://www.meicmodel.org/) with an original spatial resolution of 0.25°×0.25°. Population density was applied to relocate MEIC to each modeling domain. A high-resolution inventory that incorporates more information of local emission sources was applied for Jiangsu (JS, Zhou et al., 2017). Both MEIC and JS inventories are for 2012. The emissions for 2014 were obtained using a simple scaling method based mainly on changes in activity levels (energy consumption and

https://doi.org/10.5194/acp-2019-689
Preprint. Discussion started: 12 November 2019

Atmospheric Chemistry and Physics Discussions

industrial production, etc) between the three years. Biogenic emission inventory was from the Model Emissions of Gases and Aerosols from Nature (MEGAN, Sindelarova et al., 2014), and the emission inventories of Cl, HCl and lightning NO_X were from the Global Emissions Initiative (GEIA, Price et al., 1997). Meteorological fields were provided by the Weather Research and Forecasting Model (WRF) version 3.4, a state-of-the-art atmospheric modeling system designed for both meteorological research and numerical weather prediction (http://www2.mmm.ucar.edu/wrf/users/), and the carbon bond gas-phase mechanism (CB05) and AERO5 aerosol module were adopted. Other details on model configuration and parameters were given in Zhou et al. (2017). The simulations were conducted for January, April, July and October to represent four typical seasons in 2014. A 5-day spin-up period of each month was used to minimize the influences of initial conditions in the simulations.

Using the observation data of US National Climate Data Center (NCDC) at 43 stations in YRD (see Figure 1 for the locations of the stations), the WRF modeling performance was evaluated with statistical indicators including averages of simulations and observations, bias, normalized mean bias (NMB), normalized mean error (NME), root mean squared error (RMSE) and index of agreement (IOA). As can be found in Table S7 in the Supplement, discrepancies between simulation and observation met the criteria by Emery et al. (2001) for most cases, implying the reliability of meteorological simulation. However, bigger errors were found for the simulation of wind direction.

2.4 Ground-based and satellite observations

There were very limited continuous ground measurement data available for ambient NH_3 and NH_4^+ aerosol in the YRD region 2014, particularly at rural/remote sites that are more representative for the regional atmospheric environment. We conducted on-line hourly measurements using the MARGA (Monitor for AeRosols and Gases in ambient Air, ADI2080) at an urban site in the western downtown of Nanjing (32.03°N, 118.44°E) from August 2014. The MARGA is a state-of-art instrument which monitors near real-time water-soluble ions in aerosols and their gaseous precursors (Lanciki, 2018), and it was able to capture rapid compositional changes in $PM_{2.5}$ (Chen et al., 2017). The site was on the roof of the building of Jiangsu Provincial Academy of Environmental Science (30 m above the ground) surrounded by residential and commercial buildings and heavy traffic (JSPAES: Li et

https://doi.org/10.5194/acp-2019-689
Preprint. Discussion started: 12 November 2019

Atmospheric Chemistry and Physics Discussions

al., 2015; Chen et al., 2019). The data of October 2014 were applied in this work to evaluate the NH_3 inventories through air quality simulation. Besides, the hourly data of online measurement with MARGA were available at a suburban site in Pudong, Shanghai (SHPD) for April, July and October 2014 (unpublished data from Shanghai Environmental Monitoring Center).

Regarding satellite observation, the daily NH_3 vertical column densities (VCDs) measured through Infrared Atmospheric Sounding Interferometer (IASI) were downloaded from ESPRI data center (http://cds-espri.ipsl.upmc.fr/etherTypo/index.php?id=1700&L=1). We used the data in the domain (114.2°E-124.1°E, 26.1°N-35.4°N) with a 9:30am equator local crossing time to evaluate the NH_3 emissions. Only pixels with radiative cloud fraction<25%, relative error <100% and absolute error<5×10^{15} molec/cm^2 were used following the criteria of previous studies (van Damme et al., 2014; 2015). The monthly average VCDs for January, April, July and October 2014 were calculated and allocated into a grid system of 0.5° (longitude)×0.25° (latitude) using the Kriging interpolation method, as shown in Figure 3.

3. Results and discussions

3.1 Comparison between the two inventories

Table 2 summarizes the NH_3 emissions estimated with E1 and E2 by source category and province for the YRD region in 2014. Agricultural activities (livestock farming and fertilizer) were identified as the most important sources of NH_3, with the fraction to total emissions ranged 74-84% in the two methods. Applying the constant emission factors, E1 derived a total NH_3 emission estimate 60% larger than that by E2 that characterized the agricultural processes. In particular, emissions from agricultural activities in E1 were calculated as twice of those in E2. At the national scale, similarly, Dong et al. (2016) applied constant emission factors and estimated the total NH_3 emissions at 16.1 Tg for China, 64% larger than 9.8 Tg by Huang et al. (2012) with the agricultural processes characterized. The clearly larger estimation by constant emission factors was due mainly to the fact that most emission factor measurements were conducted in hot seasons. Among the provinces, the fraction of Jiangsu to YRD emissions was ranged 45-47% in the two methods, followed by Anhui around 37%. Agricultural activities were relatively intensive in the two provinces: Jiangsu and

https://doi.org/10.5194/acp-2019-689
Preprint. Discussion started: 12 November 2019


Atmospheric Chemistry and Physics Discussions

Anhui contributed 46% and 33% of the economic output of agriculture and livestock/poultry farming in YRD region, and the collective fraction of fertilizer use by the two provinces reached 84%. In contrast, agricultural activities were limited in Shanghai and Zhejiang, with smaller emissions estimated in both inventories.

Monthly distribution of NH_3 emissions in the two inventories were illustrated in Figure 4. Both inventories indicated relatively large emissions in summer (from June to August), and elevated emissions were also found in March and September in E2, The difference comes mainly from the effect of farming season on fertilization process. For example, the top dressing fertilization for winter wheat was conducted mostly during the seedling establishment and elongation stage in the following spring, resulting in enhanced use of nitrogen fertilizer in March. Moreover, September was the month with the highest temperature following summer in YRD 2014, and the elevated NH_3 led to large emissions in E2. Compared to fertilizer use, less variation of monthly emissions were found for livestock/poultry breeding, as very limited change in livestock amount was detected in both inventories.

Illustrated in Figure 5 are the spatial distributions of emissions from fertilizer use, livestock/poultry breeding and all categories in the two inventories. Both inventories indicated the large emission intensities in northern Jiangsu (Xuzhou and Yancheng) and northern Anhui (Fuyang, Bozhou and Suzhou) with abundant agricultural production. Xuzhou and Yancheng collectively contributed 36%, 31% and 41% of the provincial fertilizer use, agricultural economic product, and livestock/poultry farming product in Jiangsu, respectively. Similarly, Fuyang, Bozhou and Suzhou collectively contributed 36%, 36% and 35% of the provincial sown area, agricultural economic product, and livestock/poultry farming product in Anhui, respectively.

The differences in spatial pattern between the two inventories were further investigated for total and fertilizer use emissions by month, through the indicator *RD* calculated with Eq. (4). As shown in Figure 6, larger *RD* was found in northern Jiangsu, northern Anhui, and eastern Zhejiang, while smaller in western Zhejiang. The emissions in E1 were commonly larger than that in E2 across the YRD region for January and April. In contrast, larger emissions in E2 were found in northern Jiangsu (e.g., Xuzhou and Yancheng) and northern Anhui for July and October. The discrepancy resulted from the combined effect of varied activity data and emission factors as described in Section 2.2: top dressing fertilization and high temperature led to enhanced volatilization rate and thereby emissions of NH_3 in E2, and the abundant

https://doi.org/10.5194/acp-2019-689
Preprint. Discussion started: 12 November 2019


Atmospheric Chemistry and Physics Discussions

386 fertilizer use in the broad cropland in northern YRD region was the main reason for
387 the high emissions in October.

388 Figure 7 compares the NH_3 emissions by province and source category in this
389 work and other available downscaled national (MEIC) or provincial inventories in the
390 YRD region. Results from other studies were commonly ranged between E1 and E2
391 for agriculture, the most important NH_3 source. With constant emission factors
392 applied, the MEIC estimates were similar to those in E1. Most current provincial
393 inventories made some corrections for emissions from fertilizer use or
394 livestock/poultry breeding, but the local geographical and meteorological information
395 were not always fully applied in the emission estimation. For example, Liu and Yao
396 (2016) calculated the emissions from livestock/poultry breeding for Jiangsu based on
397 TAN, but did not consider the impacts of varied monthly temperatures on the
398 emissions. Zheng et al. (2016) calculated the agricultural NH_3 emissions for Anhui
399 based on a national guideline of NH_3 emission inventory development (MEP, 2014),
400 and ignored the impact of soil condition (e.g., pH) on NH_3 volatilization from
401 fertilizer use.

402 **3.2 Evaluation of the inventories with transport modeling and ground**
403 **observation**

404 Figures 8 illustrates the observed and simulated hourly concentrations for
405 gaseous NH_3 and inorganic aerosol species (NH_4^+, SO_4^{2-} and NO_3^-) in ambient
406 particles for April, July and October at SHPD and October at JSPAES. The
407 normalized mean biases (NMB) and normalized mean errors (NME) between
408 observed and simulated concentrations, and the monthly average concentrations from
409 observation and simulation are summarized in Table 3. In general, the model captured
410 the temporal variation of NH_3 concentrations, and the simulated monthly average
411 concentrations were close to the observed ones at both sites. The biggest discrepancy
412 was found at SHPD for April, where the monthly average NH_3 was simulated 56%
413 larger than observation with E1, and the smallest at JSPAES for October, where the
414 simulated was 1.7% smaller than observation with E1. The simulated temporal
415 variation, however, was much larger than the observation, leading to relatively large
416 NME, particularly at SHPD for April. Clear difference was found for the simulation
417 under two NH_3 inventories. In general, the average of simulated NH_3 concentrations
418 at the two sites for available months was 27% smaller in E2 than that in E1 (note the

https://doi.org/10.5194/acp-2019-689
Preprint. Discussion started: 12 November 2019


Atmospheric Chemistry and Physics Discussions

419 total NH_3 emissions in E2 was 38% smaller than that in E1 for the whole YRD region).
420 At SHPD site, application of E1 in CMAQ overestimated the NH_3 concentration,
421 indicated by the positive NMB values and the larger simulated concentrations than
422 observation. Such overestimation was clearly corrected when E2 was applied, and the
423 NMEs with E2 were substantially reduced as well, as shown in Table 3. The better
424 modeling performance implies the improved estimation and spatiotemporal
425 distribution of emissions. At JSPAES, air quality modeling with both inventories
426 underestimated the NH_3 concentrations, and the simulated monthly average
427 concentration with E1 was much closer to observation than that with E2. The close
428 NMEs between the two inventories indicated very limited improvement at the site, in
429 contrast to SHPD. Located in urban area, JSPAES might be largely affected by the
430 local sources like transportation and residential activities. NH_3 emissions of such
431 source categories, however, were not improved in E2.

432 To reduce the impact of highly uncertain hourly meteorology simulation and
433 emission data on air quality modeling, daily NH_3 concentrations derived from
434 simulation and observation were further compared for October at JSPAES. As
435 illustrated in Figure S3 in the supplement, better agreement between observation and
436 simulation was achieved for daily concentration than hourly, and the NMEs for E1
437 and E2 were reduced respectively from 56.9% and 53.7% to 37.0% and 32.5%,
438 respectively. Besides emission data, uncertainty in meteorology simulation also
439 contributed to the discrepancy between simulation and observation. For example, both
440 inventories overestimated the concentration on 7th October but underestimated that for
441 21st-22nd. In contrast to the southeasterly wind observed at ground meteorology station
442 in Nanjing, the simulated wind direction on 7th was from north, enhancing the NH_3
443 transport from Yancheng and Xuzhou in northern Jiangsu with intensive agricultural
444 activities and thereby emissions. On 21st-22nd, the underestimation NH_3 concentration
445 resulted largely from the overestimation in wind speed by WRF.

446 Compared to NH_3, the modeling performance for inorganic aerosols (NH_4^+, SO_4^{2-},
447 and NO_3^-) is better for most cases, indicated by smaller NMEs in Table 3. Some
448 exceptions exist at SHPD for NH_4^+ and SO_4^2 in October and NO_3^- in January.
449 Application of E2 reduced the NMEs and improved the simulation of NH_4^+ and SO_4^2
450 moderately, but there were no significant changes between the modeling results with
451 E1 and E2. The averages of simulated concentrations at the two sites for available
452 months was 7%, 3% and 12% smaller in E2 than those in E1 for NH_4^+, SO_4^{2-}, and

https://doi.org/10.5194/acp-2019-689
Preprint. Discussion started: 12 November 2019

Atmospheric Chemistry and Physics Discussions

NO_3^-, respectively, and the differences were clearly smaller than that for NH_3 at 27%. As large fraction of inorganic aerosols comes from secondary chemistry reaction, they are more representative for the regional atmosphere condition other than the local environment around the measurement site. Therefore, the air quality modeling at a horizontal resolution at 9×9 km is expected to be able to better simulate the concentrations for secondary inorganic aerosols than primary gaseous pollutants, particularly when emissions from some local sources are not sufficiently quantified. The simulated concentrations were commonly larger than observation for NH_4^+ and SO_4^{2-}, particularly at SHPD in July and October. The uncertainty of model could be an importance source of the discrepancy, as the recent reported mechanisms of gas to particle conversion were not sufficiently applied in the CMAQ we used (Wang et al., 2016; Cheng et al., 2016). In addition, positive or negative artifacts also existed in ground observation with MARGA, resulting from the unexpected reaction between acid gaseous pollutants and nitrate aerosol (Wei et al., 2015). From an emission perspective, the overestimation was partly corrected when smaller NH_3 emissions in E2 were applied instead of E1 in the model. Due to missing information on individual industrial plants, moreover, the inventory we used in CMAQ failed to fully capture the progress of emission control in YRD region and probably overestimated the SO_2 emissions (Zhang et al., 2019). The formation of sulfate ammonium aerosols could then be enhanced through the irreversible reaction between SO_2 and NH_3. The process simultaneously reduced the amount of NH_3 reacted with HNO_3, leading further to the underestimation of nitrate aerosols. As shown in Table 3, application of E2 with less NH_3 emissions than E1 could not improve the modeling performance of nitrate aerosols. The impact of SO_2 and NO_X emission on SIA modeling will be further discussed in Section 3.4.

3.3 Evaluation of the inventories with transport modeling and satellite observation

To be consistent with the local crossing time of IASI at 9:30am, the average of simulated hourly NH_3 concentrations at 9:00 am and 10:00 am were applied to calculate the NH_3 VCDs, using the following equations:

$$n_{NH3} = \sum_{k=1}^{23} m_k \times \Delta H_k \times 100 \quad (5)$$

$$\Delta H_k = H \times \ln(\frac{p_k}{p_{k+1}}) \quad (6)$$

https://doi.org/10.5194/acp-2019-689
Preprint. Discussion started: 12 November 2019


Atmospheric Chemistry and Physics Discussions

where n_{NH3} is the NH_3 VCDs from CMAQ model (molec./cm^2); m_k is the simulated NH_3 concentrations at vertical layer k in the CMAQ (molec./cm^3); $\triangle H$ is the height of layer k (m); H represents the height when the pressure of atmosphere declines to 1/e of the original value; and p is the air pressure. Figure 9 illustrates the simulated NH_3 VCDs with E1 and E2 for January, April, July, and October. Similar spatial patterns are found with the two inventories, i.e., relatively large NH_3 VCDs were simulated mostly in northern Jiangsu and northern Anhui province, consistent with the hotspot of NH_3 emissions. The simulated NH_3 VCDs with E1 were 53% larger than those with E2 across the whole YRD region, with the maximum and minimum monthly difference calculated at 73% and 31% for April and October, respectively. The NMB, NME, and spatial correlation coefficient (r) between observed and simulated VCDs, and the monthly average VCDs from observation and simulation are summarized in Table 4. Application of both inventories resulted in larger NH_3 VCDs than those from satellite observation for January and October, while simulated VCDs for April and July were smaller. Besides the uncertainty from monthly distribution of NH_3 emissions, the bias from WRF modeling on temperature might also contribute to the discrepancy between simulated and observed VCDs. As shown in Table S7 in the supplement, WRF overestimated the monthly temperature in January and October with the NMBs calculated at 26.6% and 0.34%, and underestimated it in April and July with the NMBs calculated at-1.62% and -2.51%. Compared to E1, application of E2 significantly reduced the NMEs from 83.8% to 37.5% for January and largely corrected the overestimation in VCD simulation for January and October. The simulated VCDs were 4.3% larger and 1.4% smaller than observation for the two months, respectively. The results implied satisfying agreement between the simulated and observed VCDs over the YRD region. Improvement in NH_3 VCD simulation was also found for April when E2 instead of E1 was applied in the air quality modeling, with the NMEs reduced from 65.8% to 60.7%. For July, however, application of E2 did not improve the model performance, implying that current method in E2 could possibly underestimate the NH_3 volatilization when the actual ambient temperature was high. Besides emissions, the discrepancy could result from various factors including the uncertainty in chemical mechanisms in CMAQ and environmental condition. Errors from satellite retrieval could also contribute to the inconsistence between simulation and observation. van Damme et al. (2014), for example, estimated an error of 19% for the total NH_3 columns in Asia. As IASI does not provide the

https://doi.org/10.5194/acp-2019-689
Preprint. Discussion started: 12 November 2019


Atmospheric Chemistry and Physics Discussions

averaging kernel moreover, uncertainty in NH_3 column retrieval could result from the reduced sensitivity of satellite measurement towards the surface.

To further investigate the impact of soil pH on the emissions and thereby the modeling performance on NH_3 VCDs, the soil in the YRD region was classified to three types, acidic soil (pH≤6.5), neutral soil (6.5<pH≤7.5), and alkali soil (pH>7.5), and the NMB and NME between the simulated and observed NH_3 VCDs were calculated by soil type and month, as summarized in Table 5. For neutral and acidic soil, application of E2 that considers the effect of farming season, geophysical condition and manure management on NH_3 emission rates resulted in clearly smaller NMEs than E1, implying the improvement in emission estimation. For acidic soil, however, the NMBs were negative for all the months when E2 was applied, and the NMEs were elevated compared to E1 except for January. Moreover, application of E2 resulted in negative NMBs for neutral and alkali soil in April and July as well. Those results implied that E2 possibly underestimated the NH_3 emissions for acidic soil particularly for warm seasons. With the correction of pH and temperature, the NH_3 volatilization rate from basal dressing fertilization was relatively low, indicating that the current near-linear assumption between the soil pH and NH_3 volatilization rate might not be appropriate for soil with low pH values for eastern China. As shown in Figure S4 in the supplement, the measured NH_3 volatilization rates from urea and ABC fertilizer use under relatively high soil pH (Zhang et al., 2002; Zhong et al., 2006) were close to the estimated values in E2, but the measured results for acidic soil were clearly larger than those in E2.

3.4 Impacts of SO_2 and NOx emission estimates on simulated NH_3 and aerosols

Besides meteorology condition, NH_3 emissions, and soil pH, the estimates of SO_2 and NO_X emissions could influence the NH_3 and SIA simulation as well. SO_2 can be transformed to S (IV) through liquid phase reaction and then be oxidized to S (VI) by O_3, or can be directly oxidized to H_2SO_4 by H_2O_2 or hydroxyl radical (• OH). HNO_3 can be formed through NO_2 oxidation by •OH at daytime, or through hydrolysis of N_2O_5 at aerosol surface at night. Normally NH_3 preferentially reacts with H_2SO_4 and relatively stable $(NH_4)_2SO_4$ is produced, while NH_4NO_3 could easily be decomposed under high temperature or low humidity condition. Therefore, ambient NH_3 concentrations and formation of NH_4^+ aerosols are influenced by the balance between acidic (SO_2 and NO_X) and alkaline component (NH_3) emissions.

https://doi.org/10.5194/acp-2019-689
Preprint. Discussion started: 12 November 2019

Atmospheric Chemistry and Physics Discussions

As described in Section 2.3, the SO_2 and NO_X emissions for 2014 used in this work were scaled from those for 2014 based on the changes in activity data. Ignorance of emission control progress during 2012-2014 would probably result in overestimation in emissions. The bias was evaluated through satellite observation. The daily planetary boundary layer (PBL) SO_2 and tropospheric NO_2 VCDs were obtained from the OMSO2 Level-3 product (http://disc.sci.gsfc.nasa.gov/Aura/data-holdings/OMI/omso2e_v003.shtml) and the POMINO Level-3 product from Ozone Monitoring Instrument (OMI), respectively. As shown in Table S8 in the supplement, all the provinces in YRD had their SO_2 and NO_2 VCDs substantially reduced during 2012-2014, and the VCDs declined by 48% and 31% respectively for the whole region. From a recent unpublished emission study, however, the SO_2 and NO_X emissions were estimated to reduce only 16% and 8% in the YRD region for the two years (personal communication with Cheng Huang from Shanghai Research Academy of Environmental Science). It can be inferred that, the overestimation of SO_2 emissions might enhance their reaction with NH_3 and thereby the formation of $(NH_4)_2SO_4$ in the air quality modeling. The formation of NO_3^-, in contrast, might be suppressed accordingly.

3.4.1 Identification of NH_3-rich/-poor condition in YRD region

To evaluate the non-linear relation between gaseous pollutant emissions (SO_2, NO_X and NH_3) and SIA concentrations for the YRD region, we follow Ansari and Pandis (1998) and calculated the gas ratio (GR) based on the modeling results:

$$GR = \frac{([NH_3]+[NH_4^+])-2\times[SO_4^{2-}]}{[NO_3^-]+[HNO_3]} \quad (7)$$

where the species in the bracket indicated the simulated ambient concentration. A GR smaller than 0 indicates a NH_3-poor condition, and the enhanced NH_3 emissions strengthen the oxidation of SO_2 and lead to increased SO_4^{2-} (Wang et al., 2011). A GR larger than 1 indicates an NH_3-rich condition. Enhanced NH_3 emissions have smaller effects on growth of SO_4^{2-} concentrations, and elevated SO_2 emissions may accelerate the formation of NO_3^- aerosols, as the increased NH_4^+ and SO_4^{2-} reduce the NH_4NO_3 capacity in the liquid phase (Seinfeld and Pandis, 2006). A neutral condition is judged when GR is between 0 and 1.

Figure 10 illustrates the spatial distribution of simulated GR for YRD region by month with E1 and E2 NH_3 inventories. Implied by the GR values larger than 1.0 for

https://doi.org/10.5194/acp-2019-689
Preprint. Discussion started: 12 November 2019

Atmospheric Chemistry and Physics Discussions

most of the areas, the YRD region was identified under the NH_3-rich condition when E1 was applied, except southwest Zhejiang. The judgment is consistent with previous studies (Wang et al., 2011; Dong et al., 2014). With reduced NH_3 emissions in E2, The areas under neutral or NH_3-poor condition expanded particularly for January and April. The common NH_3-rich condition suggested potentially high sensitivity of SIA formation to SO_2 and NO_X emissions.

3.4.2 Sensitivities of NH_3 and SIA to SO_2 and NOx changes

Three more cases were developed to test the effect of SO_2 and NO_X emission estimates on NH_3 and SIA simulation: Cases 1, 2 and 3 assumed 40% abatement of SO_2 emissions, 40% abatement of NO_X emissions, and 40% abatement of emissions both species, respectively. E1 was applied for NH_3 emission estimates in all the cases. Table 6 summarizes the modeling performance at JSPAES and SHPD for different cases in October. Clear changes in NH_3 and SIA simulation were found with varied SO_2 emissions, while the effect of varied NO_X emissions on air quality modeling was much smaller. The bias between simulation and observation was partly corrected for most cases, indicated by the smaller NMBs. Indicated by NMEs, however, the modeling performance was less conclusive. NMEs for NH_4^+ and SO_4^{2-} were reduced for Cases 1 and 3, while increased NMEs were found for NH_3 and NO_3^-. Limitation in the mechanisms of secondary aerosol formation can be an important reason for the discrepancy. Under NH_3-rich condition, abatement of SO_2 emissions (Case 1) would reduce the formation of $(NH_4)_2SO_4$, and thereby lead to growth of NH_3 concentrations. This is consistent with the situation in North China Plain, another typical region suffering aerosol pollution in China (Liu et al., 2018). The simulated NH_3 were 10.1% and 11.7% larger than those in base case at JSPAES and SHPD, and the simulated SIA (NH_4^++SO_4^{2-}+NO_3^-) were 7.9% and 11.0% smaller than those in base case at JSPAES and SHPD, respectively. Based on the modeling results in Table 3, as a comparison, the simulated NH_3 concentrations with NH_3 emissions in E2 were calculated 23% and 28% smaller than those with E1 at JSPAES and SHPD for October, respectively, and the analogue number for SIA concentrations were 5% at both sites. While the estimation of NH_3 emissions played an important role on NH_3 simulation, the SO_2 estimation could be more effective on SIA simulation. Abatement of NO_X emissions (Case 2) was much less influential. Less NOx slightly weakened the competition of SIA formation against SO_2, thus enhanced formation of $(NH_4)_2SO_4$ and decreased

https://doi.org/10.5194/acp-2019-689
Preprint. Discussion started: 12 November 2019


Atmospheric Chemistry and Physics Discussions

NH_3 concentration were simulated at both sites, as shown in Table 6. When SO_2 and NO_X were simultaneously reduced in the model (Case 3), similar results were found with Case 1, implying again that SO_2 could be a crucial species in SIA formation in the YRD region. In addition, NO_3^- aerosols were simulated to grow with the 40% abatement of SO_2 and NO_X emissions, and the benefits of SO_2 and NO_X control were partly weakened. To be more effective and efficient on regional air quality improvement, therefore, the control of NH_3 emissions should be strengthened along with other pollutants.

4. Conclusions

We took the YRD region in eastern China as an example and developed two inventories of NH_3 emissions for 2014 based on the constant emission factors (E1) and those characterizing the agricultural processes (E2), respectively. Available information from ground and satellite observation was applied to evaluate the inventories through air quality modeling. Both inventories indicated that agricultural activities (livestock farming and fertilizer use) were the most important sources of NH_3, but clear differences exist in estimates and spatial and seasonal distribution of NH_3 emissions. The total NH_3 emissions in E1 were estimated 60% larger than E2, and the emissions from agriculture in E1 were double of E2. The information on fertilization season and type from local investigation in E2 resulted in discrepancies in monthly distributions of NH_3 emissions from E1, particularly in northern Yangtze River Delta areas with abundant croplands. Differences in emission estimates lead to varied NH_3 concentrations from CMAQ modeling. At the suburban SHPD site, the overestimation in NH_3 concentration from CMAQ with E1 could be largely corrected with E2, implying the improved estimation of NH_3 emissions by E2. At the urban site JSPAES, however, very limited improvement was achieved when E1 was replaced by E2 in the model, indicating that the emission estimation of local urban sources like transportation and residential activities were not improved in E2. Compared to NH_3, the modeling performance for inorganic aerosols is better for most cases, and differences between the simulated concentrations with E1 and E2 were clearly smaller. Application of E2 improved the simulation of NH_4^+ and SO_4^{2-} moderately. For the comparison with satellite-derived NH_3 column, application of E2 significantly corrected the overestimation in VCD simulation for January and October with E1, but

https://doi.org/10.5194/acp-2019-689
Preprint. Discussion started: 12 November 2019

Atmospheric Chemistry and Physics Discussions

did not improve the model performance for July. Combining the soil distribution, it can be inferred that current method might underestimate the NH_3 volatilization for acidic soil particularly in warm seasons. Judged by simulated GR, most of YRD region was identified as an NH_3-rich condition except southwest Zhejiang. Through sensitivity test in which SO_2 and NOx emissions were solely or simultaneously reduced, estimation of SO_2 emissions was detected to be more effective on SIA simulation compared to NH_3. Reduced SO_2 emissions would suppress the formation of $(NH_4)_2SO_4$, and thereby lead to growth of NH_3 concentrations. The control of NH_3 emissions should be strengthened along with that of SO_2 and NO_X for improving the air quality more effectively and efficiently in the region.

This work is a tentative effort on NH_3 emission evaluation at regional scale. Given the insufficient field measurements, the relation between environmental conditions (e.g., temperature and soil pH) and NH_3 volatilization were not well quantified, resulting in bias in emission estimation. Uncertainties come also from the limitations in ground and satellite observation and incomplete mechanism of SIA formation in current air quality model. For better understanding the role of NH_3 emissions in regional air quality, more measurements on both sources and ambient concentrations are recommended in the future.

Data availability

The Multi-resolution Emission Inventory for China used in this study was obtained at http://www.meicmodel.org/ (last access: 31 July 2019, Tsinghua University, 2012). The high-resolution inventory for Jiangsu province was obtained in Zhou et al. (2017) and can be accessed at http://www.airqualitynju.com/ (last access: 31 July 2019). The daily NH_3 VCDs measured through IASI was obtained from ESPRI data center at http://cds-espri.ipsl.upmc.fr/etherTypo/index.php?id=1700&L=1 (last access: 31 July 2019). The two NH_3 emission inventories developed in this work (E1 and E2) will be available with the publication of this paper at http://airquality.nju.com.

https://doi.org/10.5194/acp-2019-689
Preprint. Discussion started: 12 November 2019

Atmospheric Chemistry and Physics Discussions

Author contributions

YZ developed the strategy and methodology of the work and wrote the draft. MY ran the model and produced the figures. XH revised the method and provided useful comments. FC and JZ conducted ground observation of NH_3 and aerosols.

Competing interests

The authors declare that they have no conflict of interest.

Acknowledgements

This work was sponsored by Natural Science Foundation of China (91644220 and 41575142) and the National Key Research and Development Program of China (2017YFC0210106). We would like to acknowledge Qizhen Liu and Zhong Zou from Shanghai Environmental Monitoring Center and Yunhua Chang from Nanjing University of Information Science & Technology for the ground measurement data, Qiang Zhang from Tsinghua University and Cheng Huang from Shanghai Research Academy of Environmental Science for emission data, and Simon Whitburn from Université Libre de Bruxelles and Yuanhong Zhao from Peking University for satellite data processing.

References

Ansari, A. S. and Pandis, S. N.: Response of inorganic PM to precursor concentrations. Environ. Sci. Technol., 32, 2706-2714, 1998.

Beusen, A. H. W., Bouwman, A. F., Heuberger, P. S. C., van Drecht, G., van der Hoek, K. W.: Bottom-up uncertainty estimates of global ammonia emissions from global agricultural production systems. Atmos. Environ., 42, 6067-6077, 2008.

Chen, D., Zhao, Y., Lyu, R., Wu, R., Dai, L., Zhao, Y., Chen, F., Zhang, J., Yu, H., Guan, M.: Seasonal and spatial variations of optical properties of light absorbing carbon and its influencing factors in a typical polluted city in Yangtze River Delta, China. Atmos. Environ., 199, 45-54, 2019.

Chen, X., Walker, J. T., Geron, C.: Chromatography related performance of theMonitor for AeRosols and GAses in ambient air (MARGA): laboratory and field-based evaluation, Atmos. Meas. Tech, 10, 3893-3908, 2017.

Cheng, Y., Zheng, G., Wei, C., Mu, Q., Zheng, B., Wang, Z., Gao, M., Zhang, Q., He, K., Carmichael, G., Poschl, U., Su, H.: Reactive nitrogen chemistry in aerosol water as

https://doi.org/10.5194/acp-2019-689
Preprint. Discussion started: 12 November 2019

714 a source of sulfate during haze events in China, Sci. Adv., 2, e1601530, doi:
715 10.1126/sciadv.1601530, 2016.

716 Cheng, Z., Wang, S.X., Fu, X., Watson, J.G., Jiang, J., Fu, Q., Chen, C., Xu, B., Yu, J.,
717 Chow, J.C., and Hao, J.: Impact of biomass burning on haze pollution in the Yangtze
718 River delta, China: a case study in summer 2011, Atmos. Chem. Phys., 14, 4573-4585,
719 2014.

720 Dong, W., Xin, J., Wang, S.: Temporal and spatial distribution of anthropogenic
721 ammonia emissions in China: 1994–2006, Environ. Sci., 31, 1457–1463, 2010 (in
722 Chinese).

723 Dong, X., Li, J., Fu, J. S., Gao, Y., Huang, K., Zhuang, G.: Inorganic aerosols
724 responses to emission changes in Yangtze River Delta, China. Sci. Total Environ., 481,
725 522-532, 2014.

726 Guo, H., Cheng, T., Gu, X., Wang, Y., Chen, H., Bao, F., Shi, S. Y., Xu, B. R., Wang,
727 W. N., Zuo, X., Zhang, X. C., Meng, C.: Assessment of $pm_{2.5}$ concentrations and
728 exposure throughout china using ground observations, Sci. Total Environ., 1024,
729 601-602, 2017.

730 Emery, C., Tai, E., Yarwood, G.: Enhanced meteorological modeling and
731 performance evaluation for two Texas episodes, Report to the Texas Natural
732 Resources Conservation Commission, prepared by ENVIRON, International Corp,
733 Novato, CA, 2001.

734 European Environment Agency (EEA): EMEP/CORINAIR Emission Inventory
735 Guidebook-2013, available at:
736 http://www.eea.europa.eu//publications/emep-eea-guidebook-2013 (last access: 9
737 March 2019), 2013.

738 Fang, X., Shen, G., Xu, C., Qian, X., Li, J., Zhao, Z., Yu, S., Zhu, K.: Agricultural
739 ammonia emission inventory and its distribution characteristics in Shanghai, Acta
740 Agriculturae Zhejiangensis, 27, 2177-2185, 2015 (in Chinese).

741 Fu, X., Wang, S., Xing, J., Zhang, X., Wang, T., Hao, J.: Increasing ammonia
742 concentrations reduce the effectiveness of particle pollution control achieved via SO_2
743 and NO_X emissions reduction in east China. Environ. Sci. Technol. Lett., 4, 221-227,
744 2017

745 Fu, X., Wang, S., Ran, L., Pleim, J. E., Cooter, E., Bash, J. O., Benson, V., Hao, J.:
746 Estimating NH_3 emissions from agricultural fertilizer application in China using the
747 bi-directional CMAQ model coupled to an agro-ecosystem model. Atmos. Chem.
748 Phys., 15, 6637-6649, 2015.

749 Li, B., Zhang, J., Zhao, Y., Yuan, S., Zhao, Q., Shen, G., Wu, H.: Seasonal variation of
750 urban carbonaceous aerosols in a typical city Nanjing in Yangtze River Delta, China.
751 Atmos. Environ., 106, 223-231, 2015.

752 Liu, X., Zhang, Y., Han, W., Tang, A., Shen, J., Cui, Z., Vitousek, P., Erisman, J. W.,
753 Goulding, K., Christie, P., Fangmeier, A., Zhang, F.: Enhanced nitrogen deposition
754 over China. Nature, 494, 459-463, 2013.

755 Huang, R., Zhang, Y., Bozzetti, C., Ho, K., Cao, J., Han, Y., Daellenbach, K. R.,
756 Slowik, J. G., Platt, S. M., Canonaco, F., Zotter, P., Wolf, R., Pieber, S. M., Bruns, E.
757 A., Crippa, M., Ciarelli, G., Piazzalunga, A., Schwikowski, M., Abbaszade, G.,
758 Schnelle-Kreis, J., Zimmermann, R., An, Z., Szidat, S., Baltensperger, U., EI Haddad,

https://doi.org/10.5194/acp-2019-689
Preprint. Discussion started: 12 November 2019

Atmospheric Chemistry and Physics Discussions

I., Prevot, A. S. H.: High secondary aerosol contribution to particulate pollution during haze events in China, Nature, 514, 218-222, 2014.

Huang, X., Song, Y., Li, M., Li, J., Huo, Q., Cai, X., Zhu, T., Hu, M., Zhang, H.: A high-resolution ammonia emission inventory in China. Global Biogeochem. Cy., 26, GB1030, doi: 10.1029/2011GB004161, 2012.

Seinfeld, J. H. and Pandis, S. N.: From air pollution to climate change. Atmos. Chem. Phys., 6, 429-443, 2006.

Kang, Y., Liu, M., Song, Y., Huang, X., Yao, H., Cai, X., Zhang, H., Kang, L., Liu, X., Yan, X., He, H., Zhang, Q., Shao, M., Zhu, T.: High-resolution ammonia emissions inventories in China from 1980 to 2012, Atmos. Chem. Phys., 16, 2043–2058, 2016.

Kurokawa, J., Ohara, T., Morikawa, T., Hanayama, S., Janssens-Maenhout, G., Fukui, T., Kawashima, K., and Akimoto, H.: Emissions of air pollutants and greenhouse gases over Asian regions during 2000-2008: Regional Emission inventory in ASia (REAS) version 2, Atmos. Chem. Phys., 13, 11019-11058, 2013.

Lanciki, A.: 2060 MARGA Monitor for AeRosols and Gases in ambient Air. Metrohm Process Analytics, Switzerland, available at: https://www.metrohm.com/en/products/process-analyzers/applikon-marga/ (last access: 2 Nov, 2019), 2018.

Liu, C., Yao, L.: Agricultural ammonia emission inventory and its distribution characteristics in Jiangsu Province, Journal of Anhui Agri. Sci., 44, 70-74, 2016 (in Chinese).

Liu, M., Huang, X., Song, Y., Xu, T., Wang, S., Wu, Z., Hu, M., Zhang, L., Zhang, Q., Pan, Y., Liu, X., Zhu, T.: Rapid SO_2 emission reductions significantly increase tropospheric ammonia concentrations over the North China Plain, Atmos. Chem. Phys, 18, 17933-17943, 2018

Li, L.: The numerical simulation of comprehensive air pollution characteristics in a typical city-cluster, Ph. D thesis, Shanghai University, Shanghai, China, 2012.

Ministry of Environmental Protection (MEP), The Guideline of Emission Inventory Development for Atmospheric Ammonia, 2014 (in Chinese)

National Development and Reform Commission of China (NDRC): National data on the cost and profit of agricultural product, China Statistics Press, Beijing, 2015 (in Chinese).

Pan, Y., Tian, S., Zhao, Y., Zhang, L., Zhu, X., Gao, J., Huang, W., Zhou, Y., Song, Y., Zhang, Q., Wang, Y.: Identifying ammonia hotspots in China using a national observation network. Environ. Sci. Technol., 52, 3926-3934, 2018.

Pan, Y., Wang, Y., Tang, G., Wu, D.: Wet and dry deposition of atmospheric nitrogen at ten sites in Northern China, Atmos. Chem. Phys., 12, 6515-6535, 2012.

Paulot, F., Fan, S., Horowitz, L. W.: Contrasting seasonal responses of sulfate aerosols to declining SO_2 emissions in the Eastern US: implications for the efficacy of SO_2 emission controls, Geophys. Res. Lett., 44, 455-464, doi: 10.1002/2016GL070695, 2017.

Price, C., Penner, J., Prather, M.: NO_X from lightning, Part I: Global distribution based on lightning physics, J. Geophys. Res.-Atmos., 102, 5929-5941, doi: 10.1029/96JD03504, 1997.

https://doi.org/10.5194/acp-2019-689
Preprint. Discussion started: 12 November 2019

Atmospheric Chemistry and Physics Discussions

803 Qin, M., Wang, X., Hu, Y., Huang, X., He, L., Zhong, L., Song, Y., Hu, M. and Zhang,
804 Y.: Formation of particulate sulfate and nitrate over the Pearl River Delta in the fall:
805 Diagnostic analysis using the Community Multiscale Air Quality model. Atmos.
806 Environ., 112, 81-89, 2015.

807 Sindelarova, K., Granier, C., Bouarar, I., Guenther, A., Tilmes, S., Stavrakou, T.,
808 Müller, J.-F., Kuhn, U., Stefani, P., and Knorr, W.: Global data set of biogenic VOC
809 emissions calculated by the MEGAN model over the last 30 years, Atmos. Chem.
810 Phys., 14, 9317–9341, 2014.

811 U.S. Environmental Protection Agency (USEPA): Compilation of Air Pollutant
812 Emission Factors, available at http://www.epa.gov/ttn/chief/ap42/index.html (last
813 access: 9 March 2019), 2002.

814 van Damme, M., Clarisse, L., Dammers, E., Liu, X., Nowak, J. B., Clerbaux, C.,
815 Flechard, C. R., Galylacaux, C., Xu, W., Neuman, J. A.: Towards validation of
816 ammonia (NH_3) measurements from the IASI satellite, Atmos. Meas. Tech., 8,
817 1575-1591, 2015

818 van Damme, M., Clarisse, L., Heald, C. L., Hurtmans, D., Ngadi, Y., Clerbaux, C.,
819 Dolman, A. J., Erisman, J. W., Coheur, P. F.: Global distributions, time series and error
820 characterization of atmospheric ammonia (NH_3) from IASI satellite observations.
821 Atmos. Chem. Phys., 14, 2905-2922, 2014.

822 Warner, J. X., Dickerson, R. R., Wei, Z., Strow, L. L., Wang, Y., Liang, Q.: Increased
823 atmospheric ammonia over the world's major agricultural areas detected from space.
824 Geophys. Res. Lett, 44, 2875-2884, doi: 10.1002/2016GL072305, 2017.

825 Wang, G., Zhang, R., Gomez, M. E., Yang, L., Zamora, M. L., Hu, M., Lin, Y., Peng,
826 J., Guo, S., Meng, J., Li, J., Cheng, C., Hu, T., Ren, Y., Wang, Y., Gao, J., Cao, J., An,
827 Z., Zhou, W., Li, G., Wang, J., Tian, P., Marrero-Ortiz, W., Secrest, J., Du, Z., Zheng,
828 J., Shang, D., Zeng, L., Shao, M., Wang, W., Huang, Y., Wang, Y., Zhu, Y., Li, Y., Hu,
829 J., Pan, B., Cai, L., Cheng, Y., Ji, Y., Zhang, F., Rosenfeld, D., Liss, P. S., Duce, R. A.,
830 Kolb, C. E., Molina, M. J.: Persistent sulfate formation from London Fog to Chinese
831 haze, P Natl. Acad. SCI. USA, 113, 13630-13635, 2016.

832 Wang, S., Xing, J., Jang, C., Zhu, Y., Fu, J. S., Hao, J.: Impact assessment of ammonia
833 emissions on inorganic aerosols in east China using response surface modeling
834 technique. Environ. Sci. Technol., 45, 9293-9300, 2011.

835 Wei, L., Duan, J., Tan, J., Ma, Y., He, K., Wang, S., Huang, X., Zhang, Y.:
836 Gas-to-particle conversion of atmospheric ammonia and sampling artifacts of
837 ammonium in spring of Beijing. Science China, 45, 216-226, 2015 (in Chinese).

838 Xiao, Z. M., Zhang, Y. F., Hong, S. M., Bi, X. H., Jiao, L., Feng, Y. C., and Wang, Y.
839 Q.: Estimation of the main factors influencing haze, based on a long-term monitoring
840 Campaign in Hangzhou, China. Aerosol Air Qual. Res., 11, 873-882, 2011.

841 Yang, F., Tan, J., Zhao, Q., Du, Z., He, K., Ma, Y., Duan, F., Chen, G., Zhao, Q.:
842 Characteristics of $PM_{2.5}$ speciation in representative megacities and across China,
843 Atmos. Chem. Phys. 11, 5207-5219, 2011.

844 Yang, Y., Zhao, Y.: Quantification and evaluation of atmospheric pollutant emissions
845 from open biomass burning with multiple methods: A case study for Yangtze River
846 Delta region, China. Atmos. Chem. Phys. 19, 327-348, 2019.

https://doi.org/10.5194/acp-2019-689
Preprint. Discussion started: 12 November 2019

Atmospheric Chemistry and Physics Discussions

Yang, Z.: Estimation of ammonia emission from livestock in China based on mass-flow method and regional comparison, Master thesis, Peking University, Beijing, China, 2008.

Yu, F., Chao, N., Wu, J., Tang, G., Chen, J., Wang, H., Wu, Z.: Research on agricultural ammonia emission inventory of Zhejiang Province in 2013, Environmental Pollution & Control, 38, 41-46, 2016 (in Chinese).

Zhang, F, Chen, X., Chen, Q.: The fertilization guideline for the main crop types in China, China Agricultural University Press, Beijing, 2009 (in Chinese).

Zhang, L., Chen, Y., Zhao, Y., Henze, D. K., Zhu, L., Song, Y., Paulot, F., Liu, X., Pan, Y., Lin, Y., Huang, B.: Agricultural ammonia emissions in China: reconciling bottom-up and top-down estimates, Atmos. Chem. Phys., 18, 339-355, 2018.

Zhang, Q., Zhang, M., Yang, Y., Lu, J.: Volatilization of ammonium bicarbonate and urea in main soil of Shandong Province, Chinese Journal of Soil Science, 33, 32-34, 2002.

Zhang, X., Wu, Y., Liu, X., Reis, S., Jin, J., Dragosits, U., van Damme, M., Clarisse, L., Whitburn, S., Coheur, P. F., Gu, B.: Ammonia emissions may be substantially underestimated in China. Environ. Sci. Technol., 12089-12096, 2017.

Zhang, X., Wang, Y., Niu, T., Zhang, X., Gong, S., Zhang, Y., Sun, J.: Atmospheric aerosol compositions in China: spatial/temporal variability, chemical signature, regional haze distribution and comparisons with global aerosols, Atmos. Chem. Phys. 12, 779-799, 2012.

Zhang, Y., Bo, X., Zhao, Y., and Nielsen, C. P.: Benefits of current and future policies on emissions of China's coal- fired power sector indicated by continuous emission monitoring, Environ. Pollut., submitted, 2019.

Zhao, B., Wang, S, Wang, J, Fu, J. S., Liu, T, Xu, J, Fu, X., Hao, J: Impact of national NOx and SO_2 control policies on particulate matter pollution in China, Atmos. Environ., 77, 453–463, 2013.

Zhao, Y., Mao, P., Zhou, Y., Yang, Y., Zhang, J., Wang, S., Dong, Y., Xie, F., Yu, Y., Li, W.: Improved provincial emission inventory and speciation profiles of anthropogenic non-methane volatile organic compounds: a case study for Jiangsu, China, Atmos. Chem. Phys., 17, 7733-7756, 2017

Zhao, Y., Qiu, L., Xu, R., Xie, F., Zhang, Q., Yu, Y., Nielsen, C. P., Qin, H., Wang, H., Wu, X., Li, W., Zhang, J.: Advantages of city-scale emission inventory for urban air quality research and policy: the case of Nanjing, a typical industrial city in the Yangtze River Delta, China, Atmos. Chem. Phys., 15, 12623-12644, 2015.

Zheng, H., Cai, S., Wang, S., Zhao, B., Chang, X., and Hao, J.: Development of a unit-based industrial emission inventory in the Beijing–Tianjin–Hebei region and resulting improvement in air quality modeling. Atmos. Chem. Phys., 19, 3447–3462, 2019.

Zheng, Z., Weng, J., Wang, S., Wang, J.: Estimation of ammonia emission in Anhui Province, Journal of Anhui Agricultural Sciences, 8, 73-75, 2016 (in Chinese).

Zhong, N., Zeng, Q., Zhang, L., Liao, B., Zhou, X., Jiang, J.: Effects of acidity and alkalinity on urea transformation in soil, Chinese Journal of Soil Science, 37, 1123-1128, 2006.

https://doi.org/10.5194/acp-2019-689
Preprint. Discussion started: 12 November 2019

Atmospheric Chemistry and Physics Discussions

891 Zhou, Y., Zhao, Y., Mao, P., Zhang, Q., Zhang, J., Qiu, L, Yang, Y.: Development of a
892 high-resolution emission inventory and its evaluation and application through air
893 quality modeling for Jiangsu Province, China, Atmos. Chem. Phys., 17, 211–233,
894 2017.

https://doi.org/10.5194/acp-2019-689
Preprint. Discussion started: 12 November 2019

Atmospheric Chemistry and Physics Discussions

FIGURE CAPTIONS

Figure 1. Studying area and research domain. The blue dots and red triangles indicate the locations of 43 meteorological monitoring sites and 2 air quality monitoring sites, respectively, and the numbers of 1–41 represent the prefectural cities of Fuyang, Bozhou, Huaibei, Suzhou, Liuan, Hefei, Huainan, Bengbu, Chuzhou, Anqing, Tongling, Wuhu, Maanshan, Chizhou, Xuancheng, Huangshan, Xuzhou, Suqian, Lianyungang, Huaian, Yancheng, Yangzhou, Taizhou, Nanjing, Zhenjiang, Changzhou, Wuxi, Suzhou, Nantong, Huzhou, Jiaxing, Hangzhou, Shaoxing, Ningbo, Zhoushan, Quzhou, Jinhua, Taizhou, Lishui, Wenzhou, and Shanghai. The map data provided by Resource and Environment Data Cloud Platform are freely available for academic use (http://www.resdc.cn/data.aspx?DATAID=201).

Figure 2. Differences of fertilizer application between the two inventories in YRD ($RD = (E_1 - E_2)/(E_1 + E_2)/2$).

Figure 3. The spatial distribution of monthly average of NH_3 vertical columns over YRD region from IASI satellite observation (Unit: 10^{15} mole./cm^2).

Figure 4. Monthly NH_3 emissions from fertilizer use and livestock farming in E1 and E2.

Figure 5. Spatial distribution of NH_3 emissions from fertilizer use, livestock farming and all categories in E1 and E2.

Figure 6. Differences of NH_3 emissions from fertilizer use and all categories between the two inventories ($RD = (E_1 - E_2)/(E_1 + E_2)/2$).

Figure 7. Comparison between the estimated NH_3 emissions in this work and other studies by province and source category. "Others" indicate Fang et al. (2015), Liu and Yao (2016), Yu et al. (2016), and Zheng et al. (2016) for Shanghai, Jiangsu, Zhejiang, and Anhui, respectively.

Figure 8. The observed and simulated hourly NH_3 and SIA concentrations with the two inventories at JSPAES and SHPD sites

Figure 9. The NH_3 VCDs in the YRD region simulated with the two inventories by month.

Figure 10. The GR values in the YRD region simulated with the two inventories by month.

https://doi.org/10.5194/acp-2019-689
Preprint. Discussion started: 12 November 2019

Atmospheric Chemistry and Physics Discussions

TABLES

Table 1. Anthropogenic NH_3 emission source categories

Category	Subcategory	Category	Subcategory
Fertilizer application	urea	Fuel combustion	industrial coal combustion
	ammonium bicarbonate		industrial oil combustion
	ammonium nitrate		industrial gas combustion
	ammonium sulfate		domestic coal combustion
	compound fertilizer		domestic oil combustion
Livestock Farming	beef cattle		domestic gas combustion
	dairy cow	Biomass burning	straw burning
	horse/donkey/mule		domestic firewood
	sow		open
	hog	Transportation	light duty gasoline vehicle
	goat		heavy duty gasoline vehicle
	sheep		light duty diesel vehicle
	layer		heavy duty diesel vehicle
	laying duck		motorcycle
	broiler	Sewage and waste treatment	waste landfill
	duck		waste incineration
	goose		waste compost
	rabbit		sewage treatment
	cattle/buffalo	Industry sources	ammonium synthesis
Human being	human sweat		nitrogenous fertilizer
	human breath		phosphate fertilizer
	human excretion		coking
	baby excretion		

https://doi.org/10.5194/acp-2019-689
Preprint. Discussion started: 12 November 2019

Atmospheric Chemistry and Physics Discussions

Table 2. Two anthropogenic NH_3 emission inventories in the YRD region in 2014 (Gg)

	Method	Livestock	Fertilizer	Chemical Industry	Biomass Burning	Waste Disposal	Traffic	Fuel Combustion	Human Beings	Total
Shanghai	E_1	14.9	11.9	0.1	0.3	5.0	1.9	5.1	5.5	44.5
	E_2	6.5	9.0							33.2
Jiangsu	E_1	340.8	357.4	14.1	29.1	6.0	8.6	5.2	30.8	791.9
	E_2	145.6	257.1							496.5
Zhejiang	E_1	115.7	93.8	2.4	10.6	6.9	7.7	4.7	28.3	270.1
	E_2	37.4	49.3							147.2
Anhui	E_1	241.5	314.9	14.7	35.9	2.8	3.3	7.3	37.7	658.2
	E_2	102.3	185.9							389.9
Total	E_1	712.7	778.0	31.2	75.9	20.7	21.6	22.3	102.2	1764.7
	E_2	291.8	501.3							1067.0

https://doi.org/10.5194/acp-2019-689
Preprint. Discussion started: 12 November 2019

Atmospheric Chemistry and Physics Discussions

Table 3. Model performance statistics for concentrations of NH_3 and SIA from observation and CMAQ simulation with the two inventories at SHPD and JSPAES sites for available months.

	Indicator	SHPD_ Apr		SHPD_July		SHPD_Oct		JSPAES_Oct	
		E_1	E_2	E_1	E_2	E_1	E_2	E_1	E_2
NH_3	NMB（%）	75.11	17.02	15.62	-12.85	32.32	-5.05	1.73	-21.75
	NME（%）	141.08	103.59	88.72	78.00	98.36	76.25	56.94	53.68
	Mean sim.（μg/m^3）	7.12	4.76	10.70	8.06	7.39	5.30	7.75	5.96
	Mean obs.（μg/m^3）	4.58		9.25		5.58		7.62	
NH_4^+	NMB（%）	-8.78	-19.14	12.98	6.11	84.45	74.02	15.01	9.53
	NME（%）	40.07	40.78	64.26	61.76	100.23	91.69	42.27	40.7
	Mean sim.（μg/m^3）	6.91	6.13	7.04	6.61	7.64	7.21	10.97	10.45
	Mean obs.（μg/m^3）	7.58		6.23		4.14		9.54	
SO_4^{2-}	NMB（%）	24.08	14.05	50.86	46.84	91.92	90.41	14.38	12.53
	NME（%）	57.59	51.61	84.63	81.15	110.18	108.61	43.65	42.31
	Mean sim.（μg/m^3）	14.75	13.56	14.60	14.21	14.53	14.41	15.5	15.25
	Mean obs.（μg/m^3）	11.89		9.68		7.57		13.56	
NO_3^-	NMB（%）	-59.13	-65.20	-78.10	-94.24	29.46	12.60	-6.55	-14.18
	NME（%）	65.72	70.16	141.43	142.86	93.69	70.54	44.81	44.94
	Mean sim.（μg/m^3）	4.93	4.19	5.39	4.64	7.32	6.37	17.53	16.1
	Mean obs.（μg/m^3）	12.05		9.01		5.65		18.76	

Note: obs. and sim. indicate the results from observation and simulation, respectively. The NMB and NME were calculated using following equations (P and O indicates the results from modeling prediction and observation, respectively):

$$NMB = \frac{\sum_{i=1}^{n}(P_i - O_i)}{\sum_{i=1}^{n} O_i} \times 100\%; \quad NME = \frac{\sum_{i=1}^{n}|P_i - O_i|}{\sum_{i=1}^{n} O_i} \times 100\%$$

https://doi.org/10.5194/acp-2019-689
Preprint. Discussion started: 12 November 2019

Atmospheric Chemistry and Physics Discussions

Table 4. Model performance statistics for NH_3 VCDs from IASI observation and CMAQ simulation using two inventories by month.

	January		April		July		October	
	E_1	E_2	E_1	E_2	E_1	E_2	E_1	E_2
NMB(%)	77.02	4.29	28.49	-59.12	12.19	-34.12	29.46	-1.77
NME(%)	83.83	37.54	65.8	60.07	43.93	51.91	46.38	43.17
r(P<0.01)	0.38	0.42	0.50	0.51	0.68	0.64	0.5	0.55
Mean sim.	14.09	8.30	9.57	3.40	11.28	6.65	10.00	7.61
IASI obs.	7.96		7.54		10.23		7.72	

https://doi.org/10.5194/acp-2019-689
Preprint. Discussion started: 12 November 2019

Atmospheric Chemistry and Physics Discussions

Table 5 The NMBs and NMEs between simulated and observed NH_3 VCDs simulation by soil pH and month

pH	Statistics (%)	January		April		July		October	
		E_1	E_2	E_1	E_2	E_1	E_2	E_1	E_2
pH>7.5	NMB	114.88	28.04	81.41	-38.99	43.3	4.24	67.99	46.95
	NME	117.8	49.27	89.23	44.38	56.11	48.13	71.49	57.44
7.5<=pH<6.5	NMB	92.82	9.19	44.6	-54.14	39.27	-10.78	44.01	11.13
	NME	95.83	34.16	64.13	54.7	52.52	45.54	52.54	37.69
pH<=6.5	NMB	41.61	-11.76	1.30	-67.41	-12.43	-55.81	8.64	-25.48
	NME	54.72	36.76	60.16	68.5	34.78	56.72	35.27	43.68

https://doi.org/10.5194/acp-2019-689
Preprint. Discussion started: 12 November 2019

Atmospheric Chemistry and Physics Discussions

Table 6 The modeling performance at JSPAES and SHPD in cases with different SO_2 and NO_X emission estimates

		JSPAES			SHPD		
	Cases	Increased/ Decreased %	NMB %	NME %	Increased/ Decreased %	NMB %	NME %
NH_3	Base case		1.73	56.94		32.32	98.36
	Case 1	10.14	11.09	59.02	11.67	47.54	102.68
	Case 2	-1.17	-0.59	57.85	-0.83	29.51	96.93
	Case 3	8.48	9.29	59.64	11.12	44.92	100.94
NH_4^+	Base case		15.01	42.27		84.45	100.23
	Case 1	-8.67	5.19	39.24	-10.99	62.53	84.93
	Case 2	1.87	17.55	45.40	1.40	87.40	102.37
	Case 3	-6.95	7.33	41.85	-10.36	65.69	86.27
SO_4^{2-}	Base case		14.38	43.65		91.92	110.18
	Case 1	-17.63	-4.90	40.81	-19.59	54.30	82.62
	Case 2	2.76	18.42	43.7	1.55	94.34	112.30
	Case 3	-14.91	-1.98	39.39	-18.45	55.96	83.67
NO_3^-	Base case		-6.55	44.81		29.46	93.69
	Case 1	1.25	-5.92	44.52	6.30	37.56	92.51
	Case 2	0.86	-5.85	46.71	-0.43	34.61	98.52
	Case 3	1.85	-4.90	46.51	5.78	42.85	97.19

https://doi.org/10.5194/acp-2019-689
Preprint. Discussion started: 12 November 2019

Atmospheric Chemistry and Physics Discussions

Figure 1

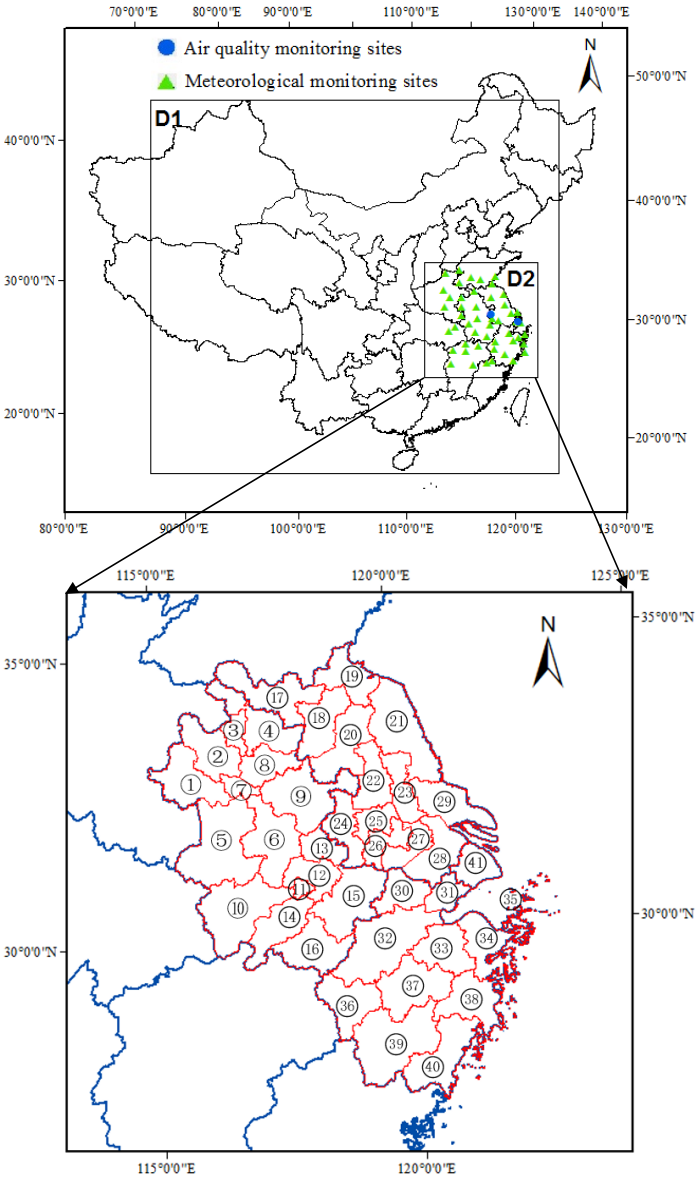

https://doi.org/10.5194/acp-2019-689
Preprint. Discussion started: 12 November 2019

Atmospheric Chemistry and Physics Discussions

Figure 2

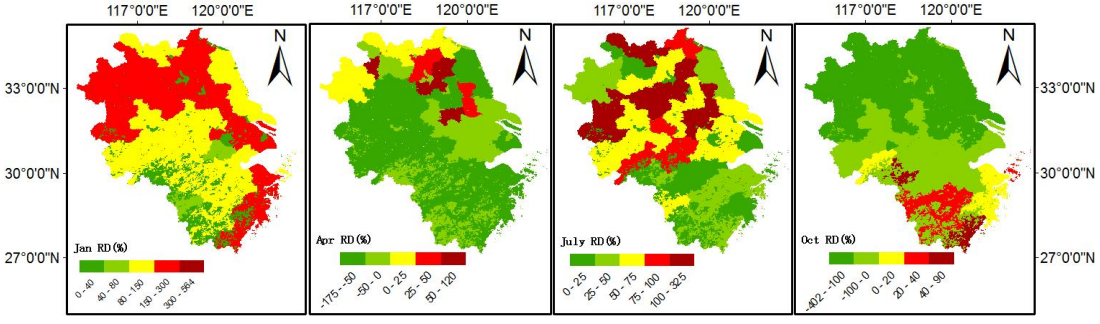

https://doi.org/10.5194/acp-2019-689
Preprint. Discussion started: 12 November 2019

Atmospheric Chemistry and Physics Discussions

Figure 3

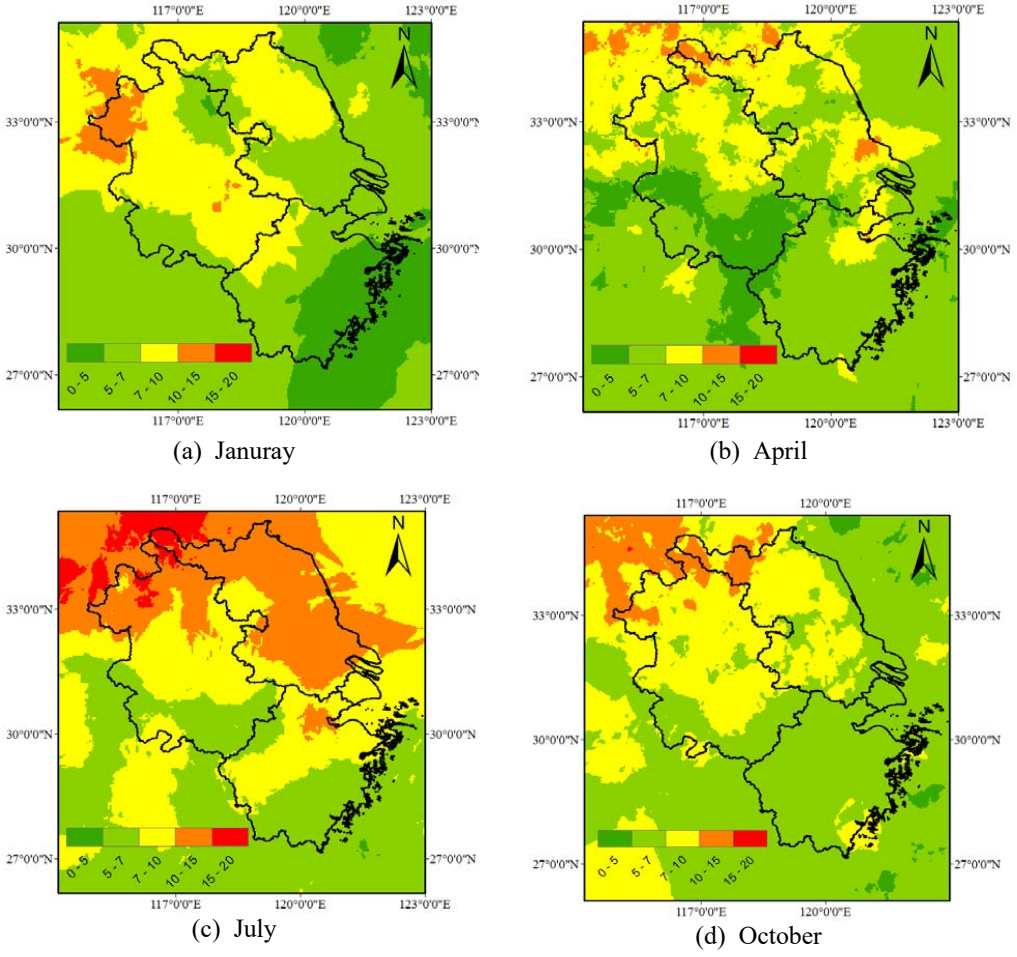

(a) Januray (b) April

(c) July (d) October

https://doi.org/10.5194/acp-2019-689
Preprint. Discussion started: 12 November 2019

Atmospheric Chemistry and Physics Discussions

Figure 4

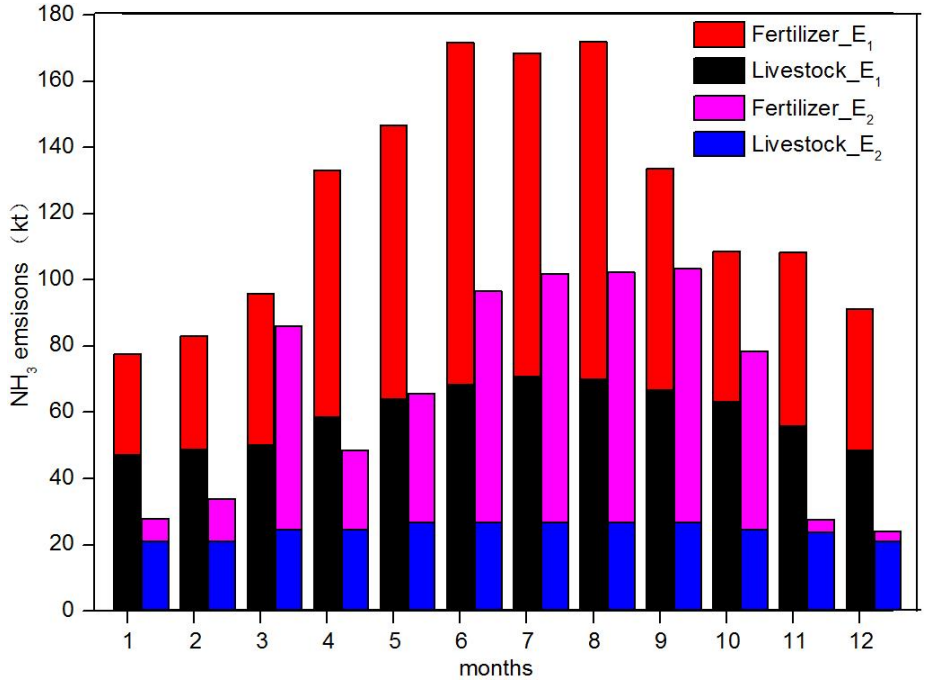

https://doi.org/10.5194/acp-2019-689
Preprint. Discussion started: 12 November 2019

Atmospheric Chemistry and Physics Discussions

Figure 5

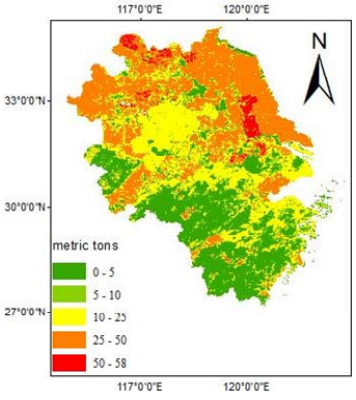

(a) Fertilizer use in E1

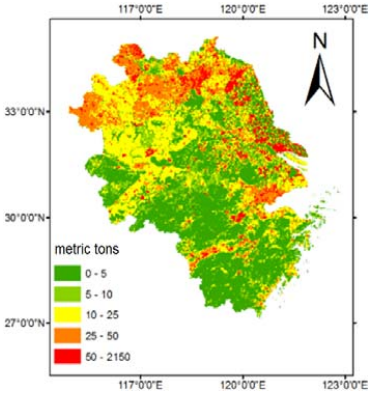

(b) Fertilizer use in E2

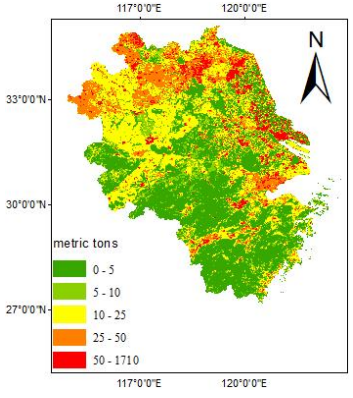

(c) Livestock farming in E1

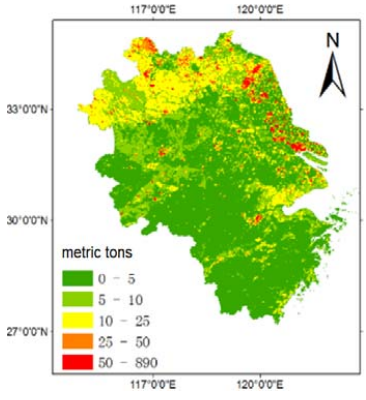

(d) Livestock farming in E2

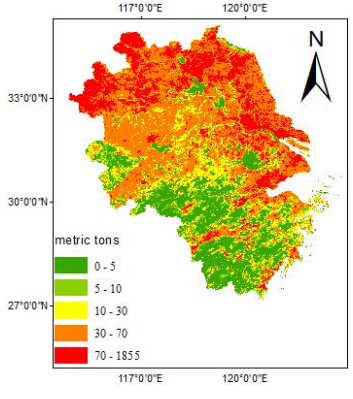

(e) Total emissions in E1

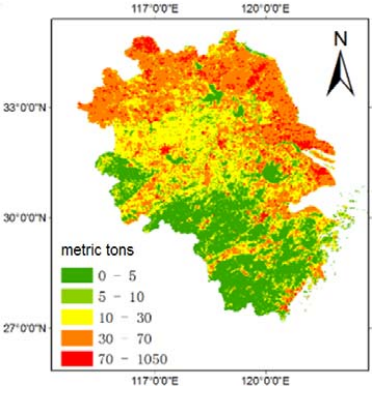

(f) Total emissions in E2

https://doi.org/10.5194/acp-2019-689
Preprint. Discussion started: 12 November 2019

Atmospheric Chemistry and Physics Discussions

Figure 6

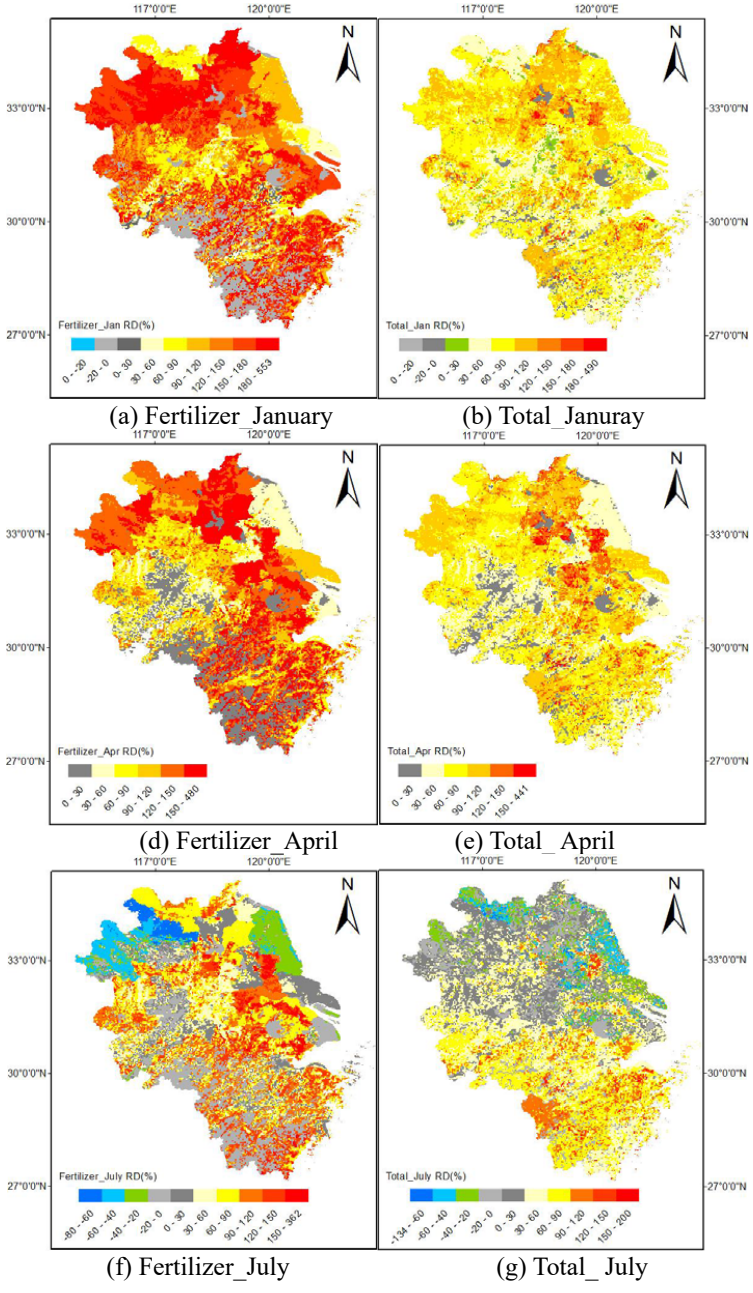

(a) Fertilizer_January (b) Total_Januray

(d) Fertilizer_April (e) Total_ April

(f) Fertilizer_July (g) Total_ July

https://doi.org/10.5194/acp-2019-689
Preprint. Discussion started: 12 November 2019

Atmospheric Chemistry and Physics Discussions

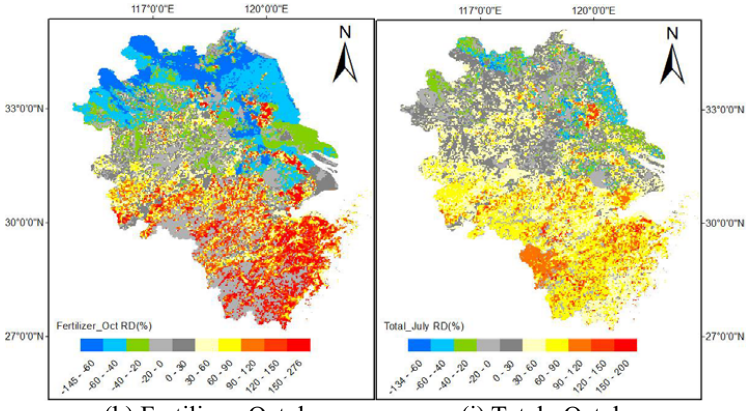

(h) Fertilizer_October (i) Total_ October

https://doi.org/10.5194/acp-2019-689
Preprint. Discussion started: 12 November 2019

Atmospheric Chemistry and Physics Discussions

Figure 7

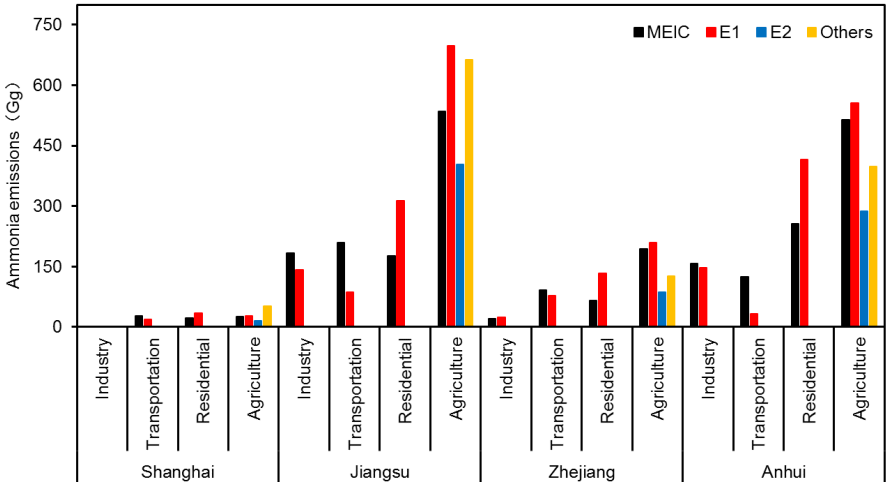

https://doi.org/10.5194/acp-2019-689
Preprint. Discussion started: 12 November 2019

Atmospheric Chemistry and Physics Discussions

Figure 8

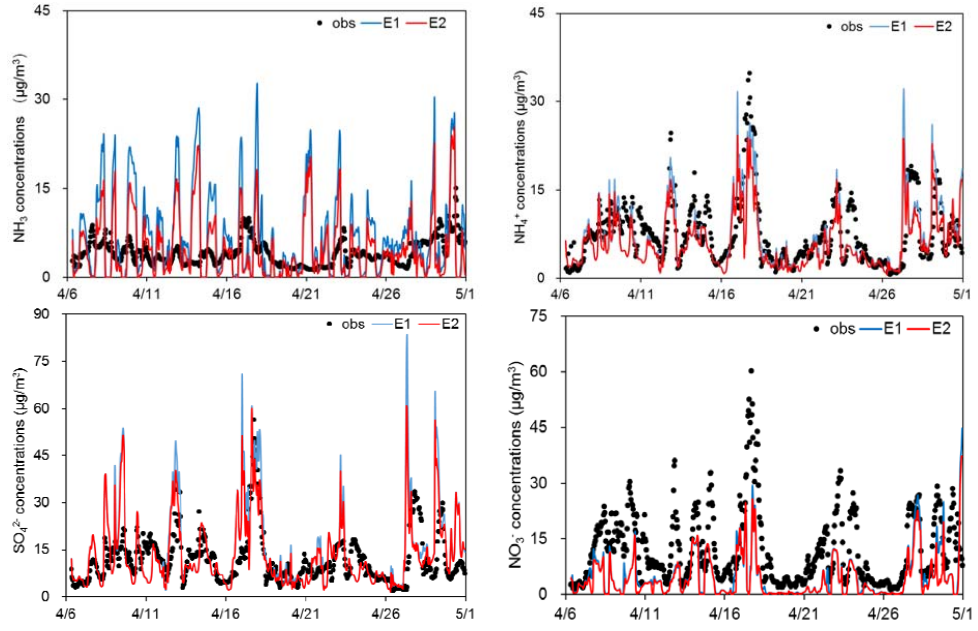

(a) SHPD_April

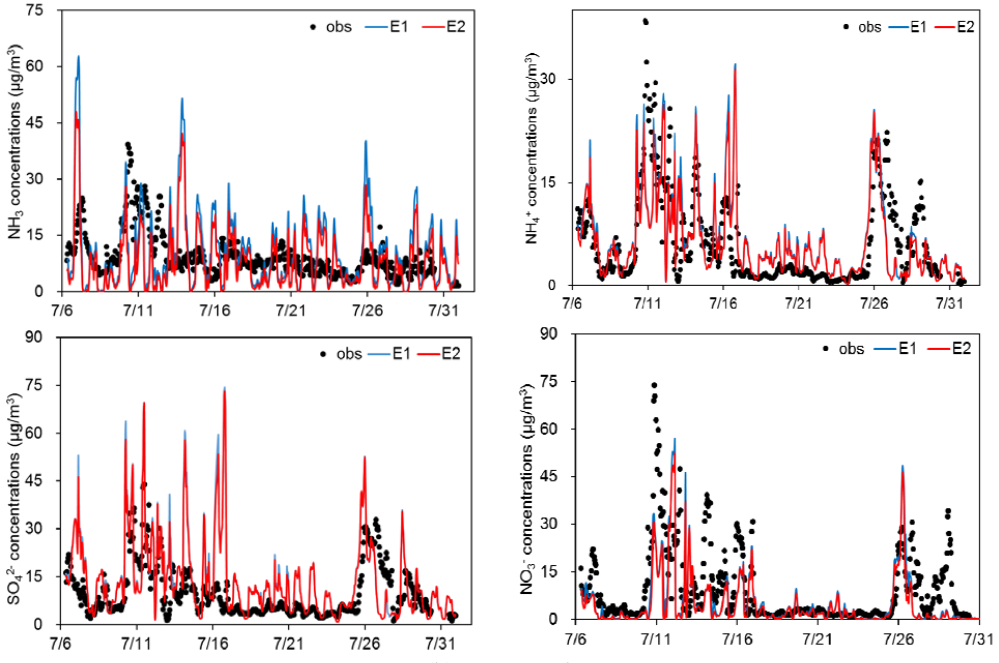

(b) SHPD_July

https://doi.org/10.5194/acp-2019-689
Preprint. Discussion started: 12 November 2019

Atmospheric Chemistry and Physics Discussions

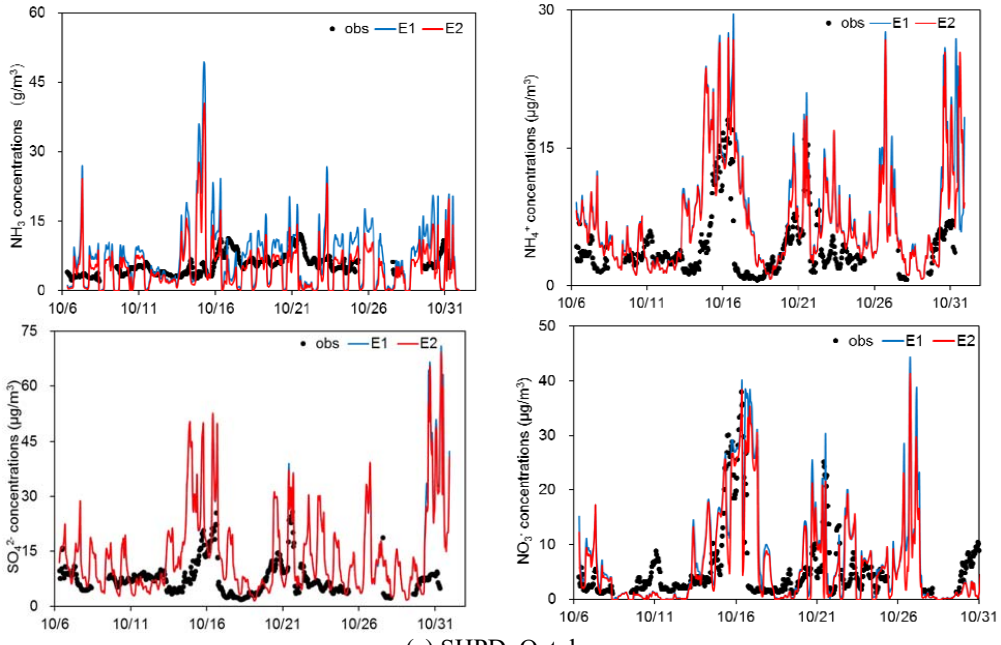

(c) SHPD_October

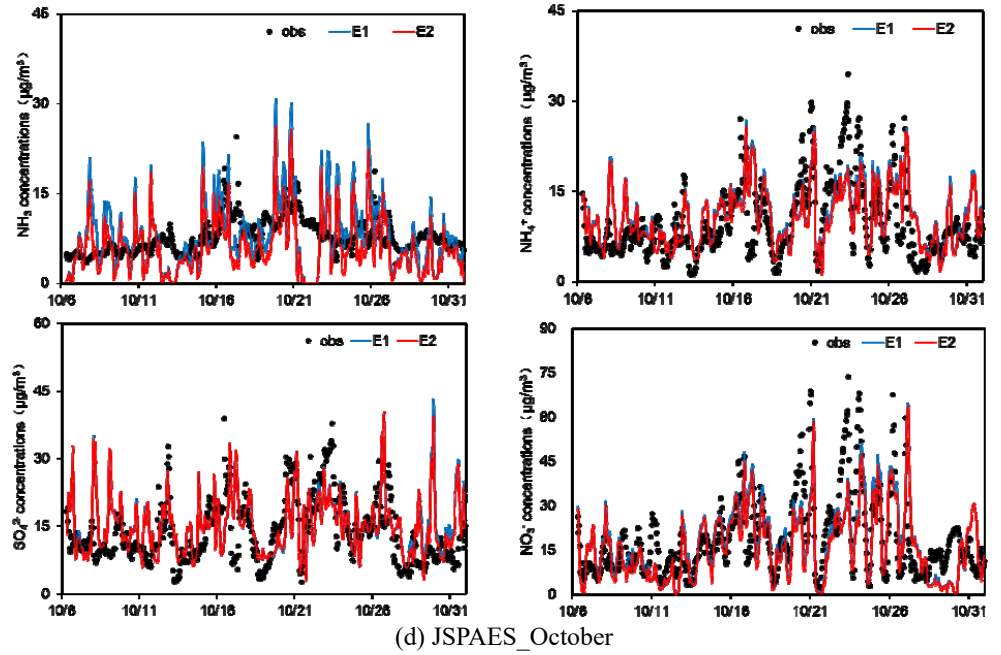

(d) JSPAES_October

https://doi.org/10.5194/acp-2019-689
Preprint. Discussion started: 12 November 2019

Atmospheric Chemistry and Physics Discussions

Figure 9

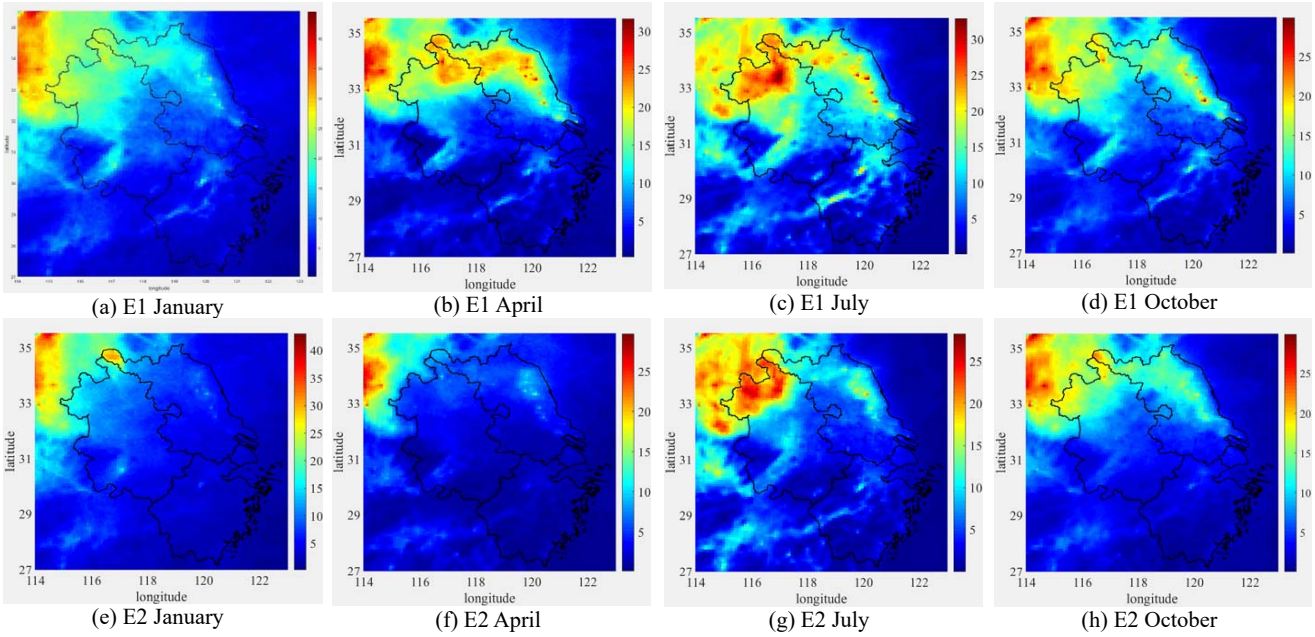

(a) E1 January (b) E1 April (c) E1 July (d) E1 October

(e) E2 January (f) E2 April (g) E2 July (h) E2 October

https://doi.org/10.5194/acp-2019-689
Preprint. Discussion started: 12 November 2019

Atmospheric Chemistry and Physics Discussions

Figure 10